nagra.

Arbeitsbericht NAB 22-03

TBO Rheinau-1-1: Data Report

Dossier X
Petrophysical Log Analysis

June 2023

S. Marnat & J.K. Becker

National Cooperative
for the Disposal of
Radioactive Waste

Hardstrasse 73
P.O. Box
5430 Wettingen
Switzerland
Tel. +41 56 437 11 11

nagra.ch

nagra.

Arbeitsbericht NAB 22-03

TBO Rheinau-1-1: Data Report

Dossier X
Petrophysical Log Analysis

June 2023

S. Marnat[1] & J.K. Becker[2]

[1] Ad Terra Energyl
[2] Nagra

Keywords:
RHE1-1, Zürich Nordost, TBO, deep drilling campaign, stochastic log interpretation, MultiMin analyses, petrophysical logs, lab data, mineralogy, clay content, clay typing, porosity

National Cooperative for the Disposal of Radioactive Waste

Hardstrasse 73
P.O. Box
5430 Wettingen
Switzerland
Tel. +41 56 437 11 11

nagra.ch

Nagra Arbeitsberichte ("Working Reports") present the results of work in progress that have not necessarily been subject to a comprehensive review. They are intended to provide rapid dissemination of current information.

This NAB aims at reporting drilling results at an early stage. Additional borehole-specific data will be published elsewhere.

In the event of inconsistencies between dossiers of this NAB, the dossier addressing the specific topic takes priority. In the event of discrepancies between Nagra reports, the chronologically later report is generally considered to be correct. Data sets and interpretations laid out in this NAB may be revised in subsequent reports. The reasoning leading to these revisions will be detailed there.

This Dossier was prepared by a project team consisting of:
S. Marnat (data analyses, interpretation and writing)
J.K. Becker (project administration and writing)

Editorial work: P. Blaser and M. Unger

The Dossier has greatly benefitted from technical discussions with, and reviews by, internal experts. Their input and work are very much appreciated.

Table of Contents

List of Tables

List of Figures

List of Appendices

List of Plates

Note: In the digital version of this report the Appendices and Plates can be found under the paper clip symbol.

Abbreviations

ANHYDR	Anhydrite weight percentage from MultiMin
APLC	Corrected neutron hydrogen index from APS (limestone matrix)
APLC_PRED	APLC prediction by MultiMin
APS	Accelerator Porosity Sonde
B/E	Barns/Electron
BS	Drilling / Coring Bit Size
CALCITE	Calcite weight percentage from MultiMin
CALI	Caliper
CARBONATES	Carbonates weight percentage from MultiMin
CHLORITE	Chlorite weight percentage from MultiMin
COAL	Coal weight percentage from MultiMin
COMPOSITE	Composite log, validated logs dataset
CONDNUM	MultiMin model condition number
CT	Conductivity in the formation
CT_PRED	CT prediction by MultiMin
CU	Capture Unit, unit for sigma
CXO	Conductivity in the invaded zone
CXO_PRED	CXO prediction by MultiMin
DENS	Bulk density
DOLOMITE	Dolomite weight percentage from MultiMin
DRHO	Bulk density correction
DRY_CLAY	Dry clay weight percentage from MultiMin
dRRC	Rush raw corrected data
DWAL_WALK2	Dry weight fraction aluminium, ECS WALK2 closure model
DWCA_WALK2	Dry weight fraction calcium, ECS WALK2 closure model
DWFE_WALK2	Dry weight fraction iron, ECS WALK2 closure model
DWFE_CORR	Dry weight fraction iron, calibrated to XRF iron content
DWSI_WALK2	Dry weight fraction silicon, ECS WALK2 closure model
DWSU_WALK2	Dry weight fraction sulphur, ECS WALK2 closure model
DWTI_WALK2	Dry weight fraction titanium from ECS, ECS WALK2 closure model

DWAL_MGWALK	Dry weight fraction aluminium, ECS MGWALK closure model
DWCA_MGWALK	Dry weight fraction calcium, ECS MGWALK closure model
DWFE_MGWALK	Dry weight fraction iron, ECS MGWALK closure model
DWK_MGWALK	Dry weight fraction potassium, ECS MGWALK closure model
DWSI_MGWALK	Dry weight fraction silicon, ECS MGWALK closure model
DWSU_MGWALK	Dry weight fraction sulphur, ECS MGWALK closure model
DWTI_MGWALK	Dry weight fraction titanium, ECS MGWALK closure model
DWMG_MGWALK	Dry weight fraction magnesium, ECS MGWALK closure model
DWAL_ALKNA	Dry weight fraction aluminium, ECS ALKNA closure model
DWK_ALKNA	Dry weight fraction potassium, ECS ALKNA closure model
DTCO	Compressional wave slowness from far monopole mid frequency source compressional wave slowness
DTCO_PRED	DTCO prediction by MultiMin
DTSM	Shear wave slowness from inline X-Dipole (90°) source
DTSM_PRED	DTSM prediction by MultiMin
ECS	Elemental Capture Spectroscopy
EDTC	Enhanced Digital Telemetry Cartridge
EMS	Environment Measurement Sonde
FE_MIN	Iron-rich minerals (Siderite, pyrite, iron oxides)
FLAG_BADHOLE_DN	Badhole flag from the Density-Neutron crossplot
FLAG_BADHOLE_OVERGAUGE	Badhole flag from the Caliper
FLAG_BADHOLE_RUGO	Badhole flag from the Density correction
FLAG_BADHOLE_STOF	Badhole flag from the Neutron stand-off
FMI	Fullbore Formation Microimager
g/cm^3	Gram per cubic centimetre
GAPI	Unit of radioactivity used for natural Gamma Ray logs
GEOLOG	Emerson software used for logs interpretation
GPCI	Geneva Petroleum Consultants International
GPIT	General Purpose Inclinometry Tool

GR	Total Gamma Ray
GR_KCOR	Total Gamma Ray corrected for mud potassium
GR_KCOR_PRED	GR_KCOR prediction by MultiMin
GOETHITE	Goethite weight percentage from MultiMin
HALITE	Halite weight percentage from MultiMin
HDAR	Hole diameter from area
HDRA	Bulk density correction
HFK	Potassium concentration from HNGS
HFK_DWK	Potassium concentration from ECS, corrected to HNGS
HI	Hydrogen Index
HNGS	Hostile Natural Gamma Ray Sonde
HRLT	High Resolution Laterolog array Tool
HSGR	HNGS Standard Gamma Ray
HTHO	Thorium concentration from HNGS
HURA	Uranium concentration from HNGS
HURA_PRED	HURA prediction by MultiMin
ILLITE	Illite weight percentage from MultiMin
KAOLIN	Kaolinite weight percentage from MultiMin
KEROGEN	Kerogen weight percentage from MultiMin
LEH.QT	Logging Equipment Head with Tension
LQC_INDEX	Log Quality Control Index
MCFL	Micro-Cylindrical Focused Log
MHF	Micro Hydraulic Fracturing
MULT_QC	MultiMin analysis quality flag
MULTIMIN	Multi mineral and multi fluid analysis module in Geolog software
m MD	Metre measured depth
MSIP	Modular Sonic Imaging Platform
NFUN	Number of MultiMin iterations
NO_K_CLAYS	Not potassic clays weight percentage from MultiMin
ORTHOCL	K-Feldspars weight percentage from MultiMin
p.u.	Porosity unit
PEFZ	Photoelectric factor
PEFZ_PRED	PEFZ prediction by MultiMin
PHI_PICNO	Core pycnometer porosity

PHI_WL1	Core water-loss porosity (105 °C) using bulk wet density
PHI_WL2	Core water-loss porosity (105 °C) using grain density
PHIE	Effective porosity
PHIT	Total porosity
PLAGIO	Plagioclases weight percentage from MultiMin
PPC	Power positioning device and caliper tool
PRECALC	Precalculation module in the Geolog software
PYRITE	Pyrite weight percentage from MultiMin
QC	Quality Control
QUALITY	MultiMin analysis quality
QUARTZ	Quartz weight percentage from MultiMin
RCL	Reduced Composite Log
RHGE_WALK2	Matrix density from elemental concentrations (WALK2 model)
RHOG	Grain density from MultiMin
RHOS	Solids density
RHOZ	Bulk density
RHOZ_PRED	RHOZ prediction by MultiMin
RT_HRLT	HRLT true formation resistivity
RUGO	Borehole wall rugosity
RXOZ	Invaded formation resistivity filtered at 18 inches
SIDER	Siderite weight percentage from MultiMin
SIGF	Macroscopic cross section for the absorption of thermal neutrons, or capture cross section, of a volume of matter, measured in capture units [c.u.]
SIGF_PRED	SIGF prediction by MultiMin
QF_SILICATES	Matrix quartz and feldspars weight percentage from MultiMin
SLB	Abbreviation for Schlumberger Logging Company
SP	Spontaneous Potential
STOF	APS Stand-Off
SWE	Effective water saturation
SWT	Total water saturation
TLD	Three-detector Lithology Density
TOC	Total organic carbon [w/w or wt.-%]
U	Photoelectric cross-section computed by Precalc [b/cc]

UBI	Ultrasonic Borehole Imager
v/v	Volume per volume
VCL	Volume of wet clay
VOL_ANHYDR	MultiMin volume of anhydrite
VOL_ANORTH	MultiMin volume of plagioclase
VOL_CALCITE	MultiMin volume of calcite
VOL_CHLOR	MultiMin volume of chlorites
VOL_DOLOM	MultiMin volume of dolomite
VOL_ILLITE	MultiMin volume of illite
VOL_ORTHOCL	MultiMin volume of potassic feldspars
VOL_SIDER	MultiMin volume of siderite
VP	Compressional waves velocity [m/s]
VS	Shear waves velocity [m/s]
VPVS	Compressional and shear waves velocity ratio
VPVS_INPUT	Array Monte-Carlo input for VP/VS
ECS WT.-%	Weight concentration
W/W	Weight per weight, concentration
WANH_WALK2	Dry weight fraction anhydrite/gypsum from ECS (WALK2 model)
WCAR_WALK2	Dry weight fraction carbonate from ECS (WALK2 model)
WCLA_WALK2	Dry weight fraction clay from ECS (WALK2 model)
WEVA_WALK2	Dry weight fraction salt from ECS (WALK2 model)
WPYR_WALK2	Dry weight fraction pyrite from ECS (WALK2 model)
WQFM_WALK2	Dry weight fraction quartz+feldspar+mica from ECS (WALK2 model)
WSID_WALK2	Dry weight fraction siderite from ECS (WALK2 model)
XRD	X-Ray Diffraction
µs/ft	Microsecond per foot (unit for sonic slowness)

1 Introduction

1.1 Context

To provide input for site selection and the safety case for deep geological repositories for radioactive waste, Nagra has drilled a series of deep boreholes ("Tiefbohrungen", TBO) in Northern Switzerland. The aim of the drilling campaign is to characterise the deep underground of the three remaining siting regions located at the edge of the Northern Alpine Molasse Basin (Fig. 1-1).

In this report, we present the results from the Rheinau-1-1 borehole located in the siting region Zürich Nordost (Fig. 1-2). In the following, the unique exploration objective of this specific borehole is further outlined.

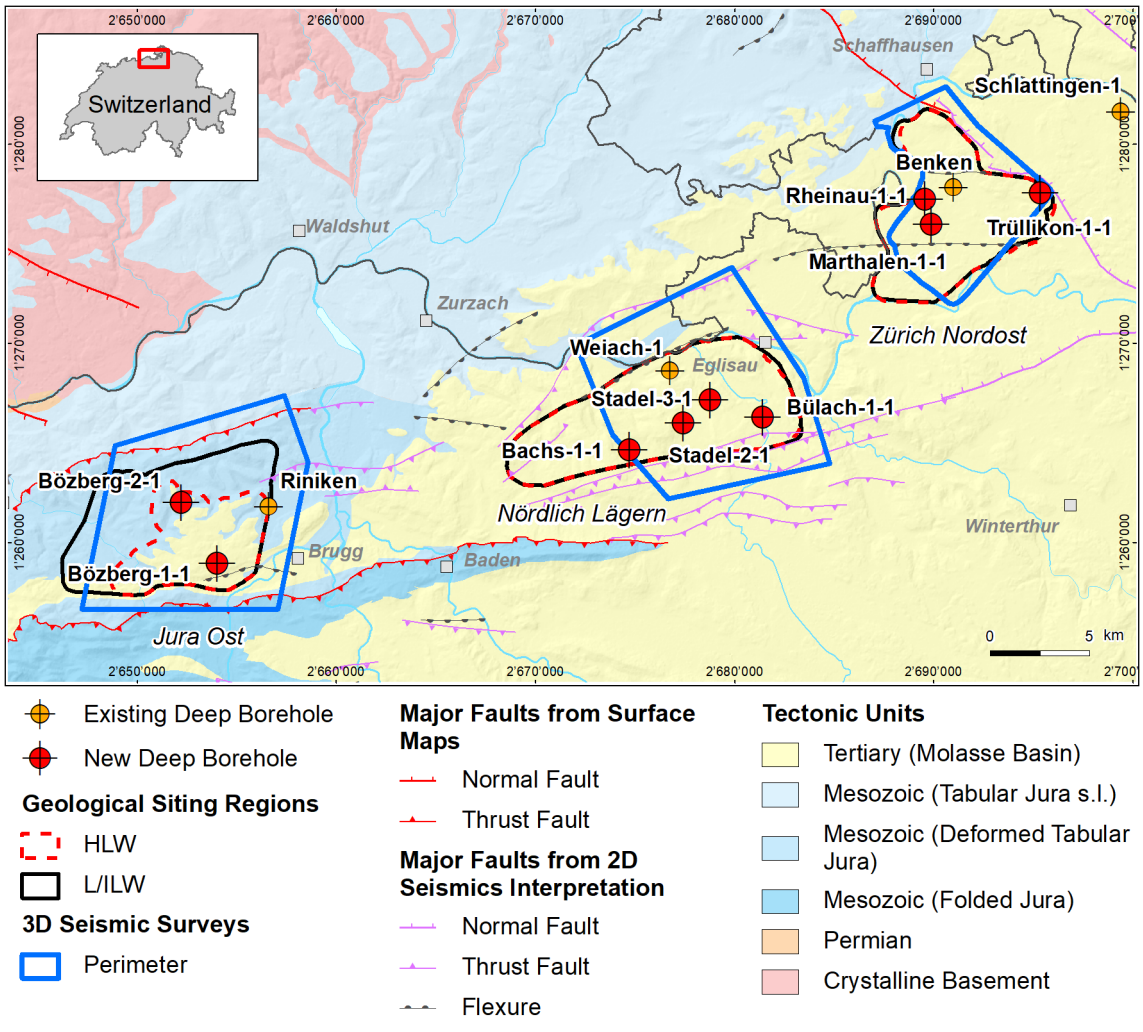

Fig. 1-1: Tectonic overview map with the three siting regions under investigation

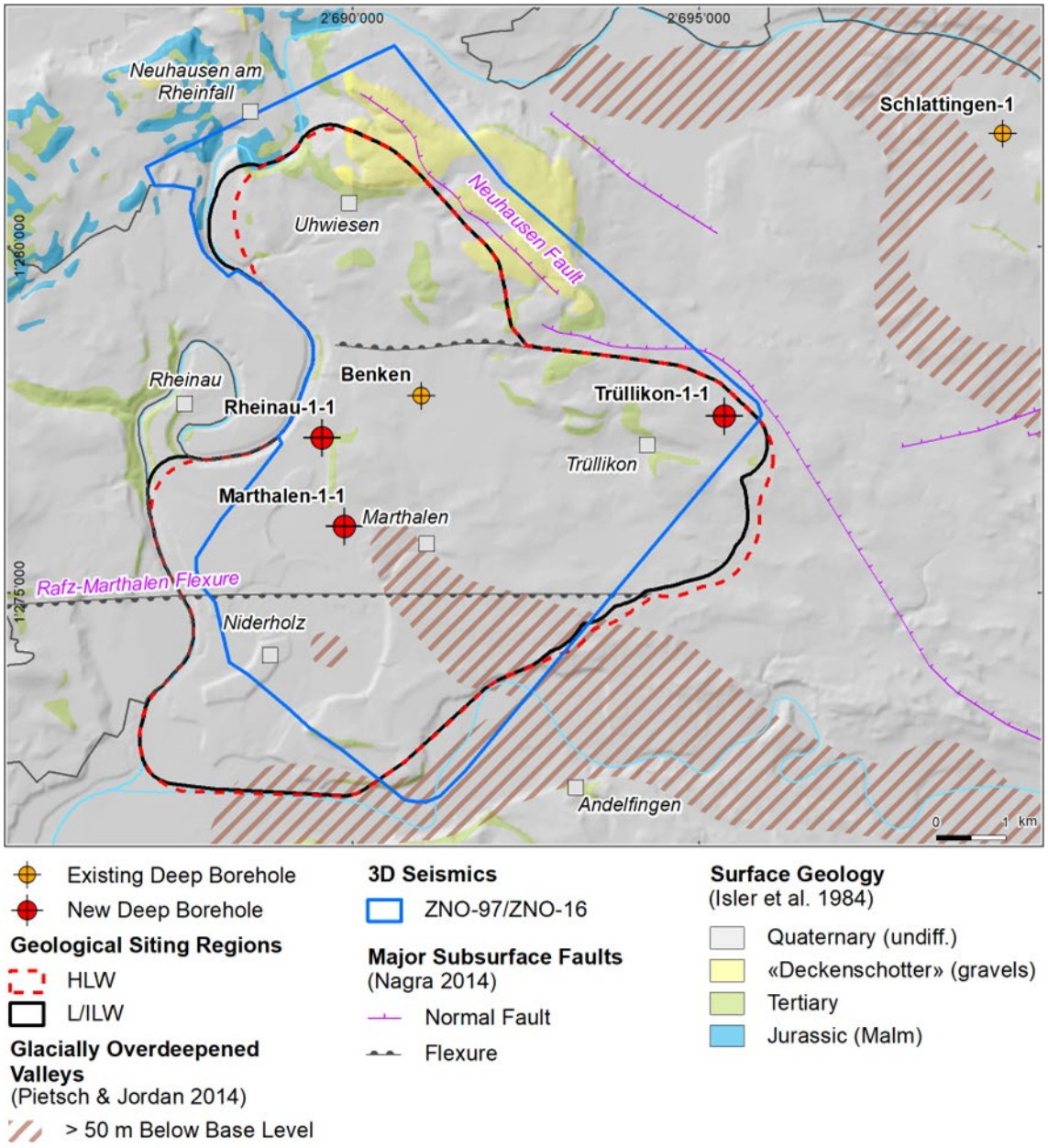

Fig. 1-2: Overview map of the investigation area in the Zürich Nordost siting region with the location of the RHE1-1 borehole in relation to the Benken, TRU1-1 and MAR1-1 boreholes

Exploration objective of the Rheinau-1-1 borehole

In the context of Nagra's TBO project, the Rheinau-1-1 (RHE1-1) borehole is the only deviated borehole. It was planned as a case study with the primary objective of characterising the structural geology of the Opalinus Clay in the area of a steeply dipping fault. Furthermore, dedicated hydrological packer testing and investigations of natural tracers in porewater were conducted to investigate the self-sealing capacity of the Opalinus Clay. More specifically, a stepped constant head injection test was performed in addition to the standard hydraulic packer test to investigate the evolution of transmissivity as a function of effective stress in a fractured interval (*cf.* Dossier VII, Hydraulic Packer Testing for details).

To enable hydraulic testing in the Opalinus Clay with its relatively low strength and high swelling capacity, the maximum borehole deviation (with respect to vertical) was limited to approximately 35° (borehole plunge of 55°). Hence, for the absolute deviation, a trade-off had to be made between maximising the lateral coverage for fracture frequency statistics (large deviation desired) and robust in-situ testing (small deviation desired).

Given the above-outlined scientific goals and related technical requirements, the Rheinau Fault, located immediately east of the Rheinau-1 drill site, was selected for this case study. It is an NNE-SSW trending, steeply dipping fault showing only very minor indications of vertical offsets in seismic amplitude sections. Nevertheless, it was already identified in seismic attribute horizon slices during initial interpretation of Nagra's 3D seismic campaign in the Zürich Nordost siting region (Birkhäuser et al. 2001) and later confirmed during the analysis of follow-up seismic processing products (e.g. Nagra 2019). Fig. 1-3 shows that this fault has a clear seismic attribute expression along the boundaries of the formations below the Opalinus Clay and also along some of the more brittle units above (see horizon slices of the Top Bänkerjoch and Top Villigen Formations shown in Fig. 1-3). However, within the Opalinus Clay, no clear seismic expression is observed. Fig. 1-4 shows the 3D seismic interpretation considered for trajectory planning of the RHE1-1 borehole together with the discussed and executed borehole trajectories.

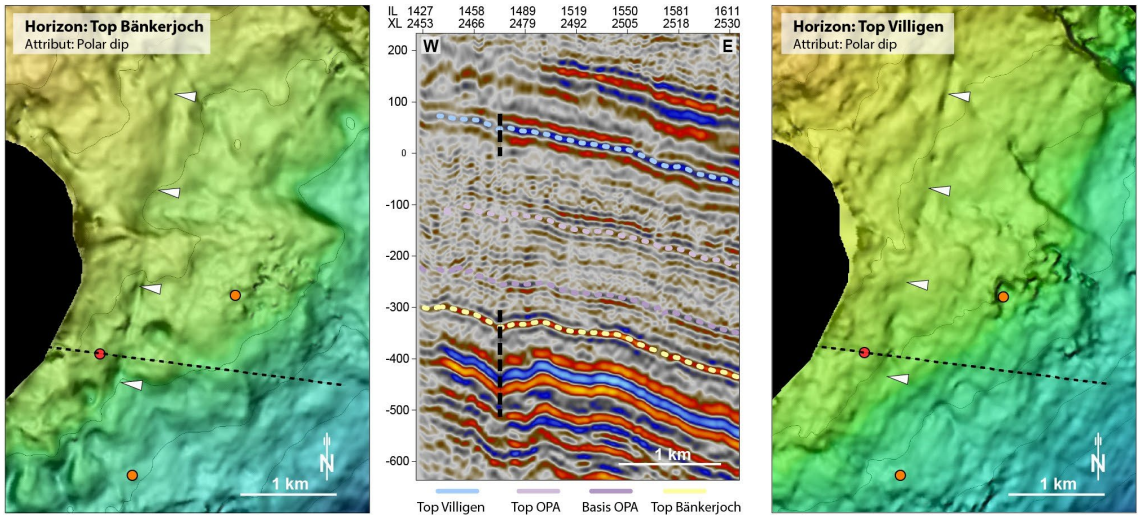

Fig. 1-3: Seismic amplitude cross-section and seismic attribute maps showing the Rheinau Fault

Left and right panels: Seismic attribute maps (polar dip) of a depth-migrated seismic cube (PSDM-A) overlain with depth values (yellowish and blueish colors indicate shallower and larger depths, respectively). The dashed black line indicates the position of the seismic section shown in the central panel. Red and orange dots show the position of the RHE1-1 borehole and neighouring boreholes, respectively. White trianlges mark the lineament representing the Rheinau Fault.

Central panel: Corresponding seismic amplitude section crossing the Rheinau Fault. The vertical axis indicates depth above sea level, and the horizontal axis shows the inline and crossline positions. The approximate trace of the Rheinau Fault above and below the Opalinus Clay is indicated by dashed black lines.

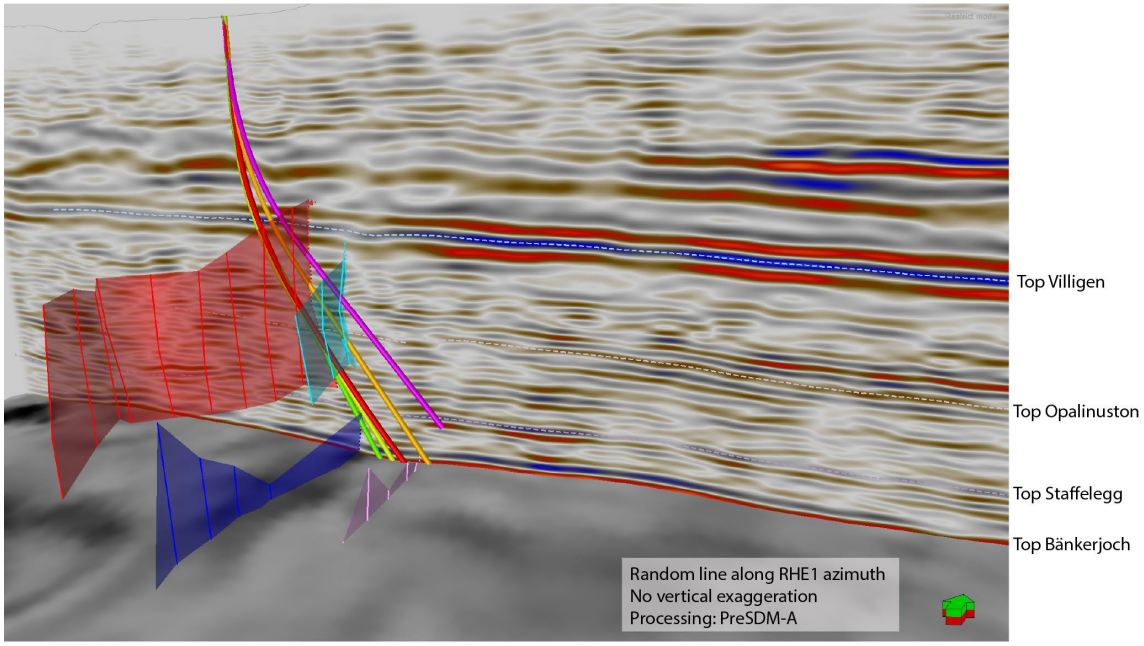

Fig. 1-4: Detailed seismic fault interpretation available for trajectory planning and discussed/ executed well trajectories

Cross-section shows seismic amplitude (seismic processing: pre-stack depth migration PDSM-A). The north direction is indicated by a green-and-red arrow. The vertical distance between the Top Opalinus Clay and Top Staffelegg is ~ 120 m and shows no vertical exaggeration. The horizon slice shows polar dip attribute. Semitransparent subvertical surfaces indicate intepreted faults. The final planned and the drilled trajectories are shown in light green and red, respectively. Other discussed trajectories are shown in yellow, orange and red.

Fig. 1-5 shows a conceptual structural model for the Rheinau Fault incorporating both 3D seismic interpretations and observations from other exploration boreholes as well as from outcrop studies. This conceptual model shows a pronounced mechanical stratigraphy of Northern Switzerland's Mesozoic sedimentary sequence with more focused deformation in the competent units, and distributed deformation in the incompetent units (Roche et al. 2020). Prior to drilling, three hypotheses were formulated on what the RHE1-1 borehole is likely to encounter in the Opalinus Clay. These hypotheses ranged from 1) absence of a distinct fault zone, likely due to a strong degree of strain partitioning within the rheologically weak Opalinus Clay, 2) one or several prominent fault zones, for example revealing cataclastic fault rock or scaly clay as it has been described to occur along larger faults within the Opalinus Clay (Jäggi et al. 2017) and 3) the former but including the occurrence of secondary mineralisations.

As this report represents a data documentation, it deliberately avoids engaging in a synthesis of the observations and test results. Nevertheless, the following results can already be highlighted:

- The drilled trajectory was within close limits compared to the planned well path (see Dossier I for a detailed comparison).
- The borehole did not yield any evidence of a larger-scale fault zone within the Opalinus Clay. However, a number of fault planes have been encountered (*cf.* Dossier V).
- In-situ hydraulic packer tests across these features (*cf.* Dossier VII) yielded hydraulic conductivities similar to undisturbed Opalinus Clay.

- The stepped constant head test demonstrated that a significant enhancement of the flow rate can only be achieved in existing fractures if the fluid pressure is raised considerably and the magnitude of elevated fluid pressure can be maintained (*cf.* Dossier VII).
- Excursions in the profiles of natural tracers can indicate past fluid flow. No such irregularities are seen for the RHE1-1 borehole in the Opalinus Clay (*cf.* Dossier VIII). The stable isotope porewater profiles show characteristics similar to the neighouring vertical boreholes MAR1-1 and Benken.

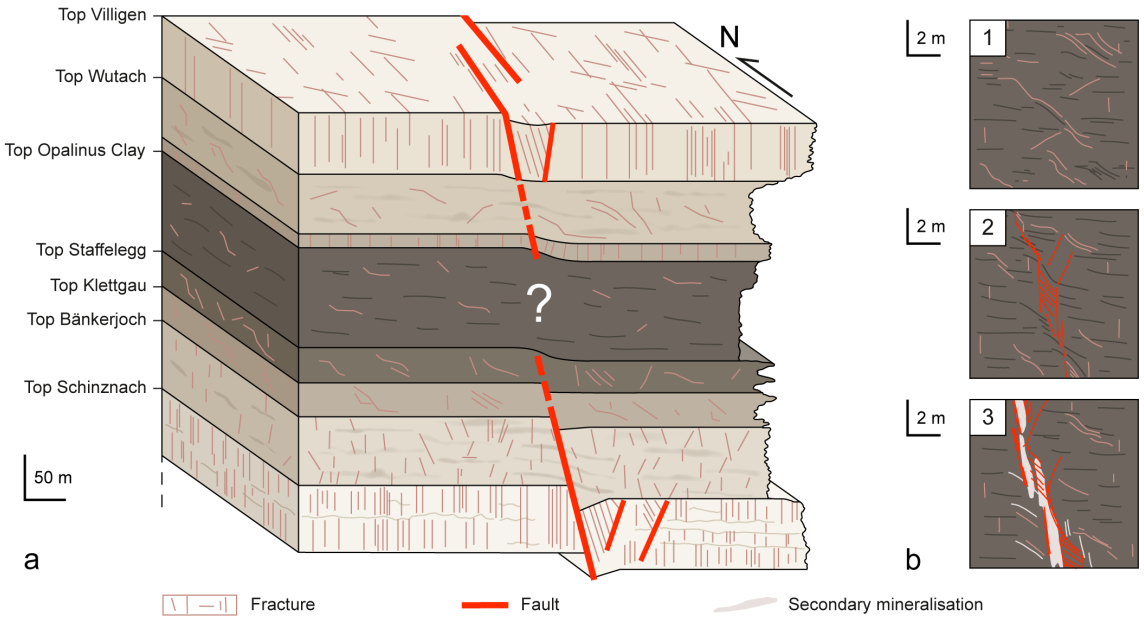

Fig. 1-5: Conceptual structural model of the Rheinau Fault

(a) Conceptual block model. The pronounced mechanical stratigraphy of the Mesozoic sequence in the area is stressed via a schematic weathering profile. The RHE1-1 borehole aimed at characterising the deformation style in the Opalinus Clay constituting a mechanically weak layer in between rheologically stiffer units (e.g. under- and overlying Schinznach/Bänkerjoch and Villigen/Wutach Formations). According to outcrop records and previous borehole results, these units show a significantly higher frequency of fault planes compared to the Opalinus Clay. In 3D seismics, the Rheinau Fault is also only clearly recognisable at the horizons related to stiffer formations.

(b) Hypothetic deformation characteristics of the Opalinus Clay to be encountered in the RHE1-1 borehole: 1) No exceptional deformation features besides small-scale fault planes as previously observed in vertical boreholes outside of seismically recognised faults. 2) One or several localised zones associated with cataclastic fault rock (e.g. scaly clay) as described for larger fault zones elsewhere (e.g. Jäggi et al. 2017). 3) The above, but also including secondary mineralisation (not to scale on picture).

1.2 Location and specifications of the borehole

The Rheinau-1-1 (RHE1-1) exploratory borehole is the eighth borehole drilled within the framework of the TBO project. The drill site is located in the western part of the Zürich Nordost siting region (Fig. 1-2). The deviated borehole reached a final depth of 827.99 m MD = 745.33 m TVD (true vertical depth)[1]. The borehole specifications are provided in Tab. 1-1.

Tab. 1-1: General information about the RHE1-1 borehole

Siting region	Zürich Nordost
Municipality	Rheinau (Canton Zürich / ZH), Switzerland
Drill site	Rheinau-1 (RHE1)
Borehole	Rheinau-1-1 (RHE1-1)
Coordinates	LV95: 2'689'563.92 / 1'277'235.06
Elevation	Ground level = top of rig cellar: 387.23 m above sea level (asl)
Borehole depth	827.99 m measured depth (MD) = 745.33 m true vertical depth (TVD) below ground level (bgl)
Borehole deviation at total depth (TD)	Inclination from vertical: 38.93° Azimuth from North: 76.25°
Drilling period	19th July – 10th October 2021 (spud date to end of rig release)
Drilling company	PR Marriott Drilling Ltd
Drilling rig	Rig-16 Drillmec HH102
Drilling fluid	Water-based mud with various amounts of different components such as[2]: 0 – 497 m: Polymers 497 – 828 m: Potassium silicate & polymers

The lithostratigraphic profile and the casing scheme are shown in Fig. 1-6. The comparison of the core versus log depth[3] of the main lithostratigraphic boundaries in the RHE1-1 borehole is shown in Tab. 1-2.

[1] Measured depth (MD) refers to the position along the borehole trajectory, starting at ground level, which for this borehole is the top of the rig cellar. For a perfectly vertical borehole, MD below ground level (bgl) and true vertical depth (TVD) are the same. In all Dossiers depth refers to MD unless stated otherwise.

[2] For detailed information see Dossier I.

[3] Core depth refers to the depth marked on the drill cores. Log depth results from the depth observed during geophysical wireline logging. Note that the petrophysical logs have not been shifted to core depth, hence log depth differs from core depth.

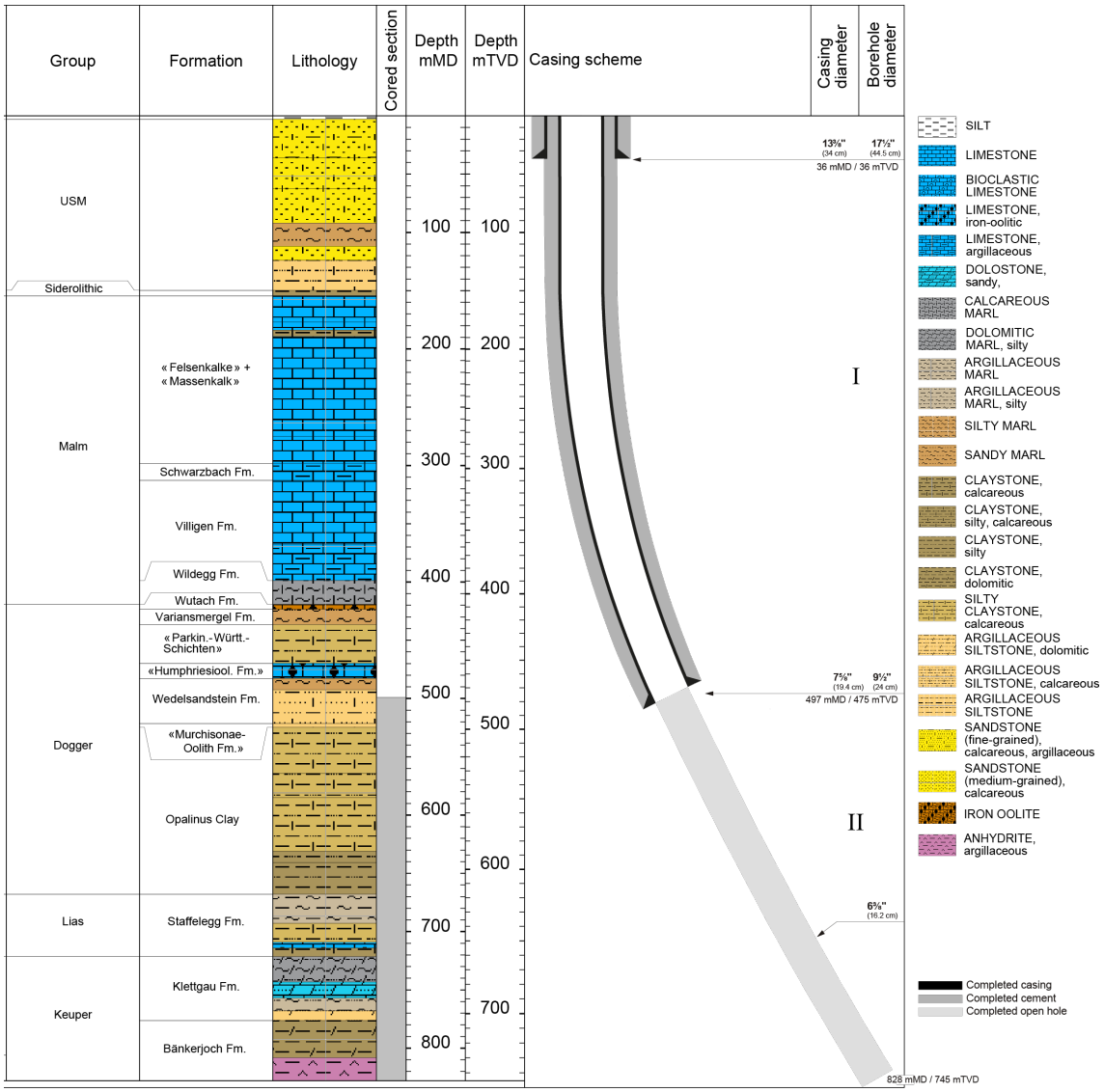

Fig. 1-6: Lithostratigraphic profile and casing scheme for the RHE1-1 borehole[4]

[4] For detailed information see Dossier I and III.

Tab. 1-2: Core and log depth for the main lithostratigraphic boundaries in the RHE1-1 borehole[5]

System / Period	Group	Formation		Core top depth in m (MD)	Log top depth in m (MD)		Core top depth in m (TVD)	Log top depth in m (TVD)	
Quaternary				**3**		—	**3**		–
Paleogene + Neogene	USM			149.90		—	149.88		–
	Siderolithic			**154.40**		—	**154.37**		–
Jurassic	Malm	«Felsenkalke» + «Massenkalk»		298.10		—	295.71		–
		Schwarzbach Formation		312.70		—	309.70		–
		Villigen Formation		398.80		—	389.75		–
		Wildegg Formation		419.20		—	408.04		–
	Dogger	Wutach Formation		423.40		—	411.78		–
		Variansmergel Formation		436.60		—	423.47		–
		«Parkinsoni-Württembergica-Sch.»		469.80		—	452.23		–
		«Humphriesioolith Formation»		482.80		—	463.20		–
		Wedelsandstein Formation		521.43	521.21	—	495.83	495.64	–
		«Murchisonae-Oolith Formation»		524.61	524.33	—	498.51	498.27	–
		Opalinus Clay		668.07	668.19	—	617.65	617.75	–
	Lias	Staffelegg Formation		**721.46**	**721.50**	—	**660.95**	**660.98**	–
Triassic	Keuper	Klettgau Formation		776.42	776.79	—	704.82	705.11	–
		Bänkerjoch Formation	final depth	827.99	828.24		745.33	745.52	

[5] For details regarding lithostratigraphic boundaries see Dossier III and IV; for details about depth shifts (core goniometry) see Dossier V.

1.3 Documentation structure for the RHE1-1 borehole

NAB 22-03 documents the majority of the investigations carried out in the RHE1-1 borehole, including laboratory investigations on core material. The NAB comprises a series of stand-alone dossiers addressing individual topics and a final dossier with a summary composite plot (Tab. 1-3).

This documentation aims at early publication of the data collected in the RHE1-1 borehole. It includes most of the data available approximately one year after completion of the borehole. Some analyses are still ongoing and results will be published in separate reports.

The current borehole report will provide an important basis for the integration of datasets from different boreholes. The integration and interpretation of the results in the wider geological context will be documented later in separate geoscientific reports.

Tab. 1-3: List of dossiers included in NAB 22-03

Black indicates the dossier at hand.

Dossier	Title	Authors
I	TBO Rheinau-1-1: Drilling	M. Ammen & P.-J. Palten
II	TBO Rheinau-1-1: Core Photography	D. Kaehr & M. Gysi
III	TBO Rheinau-1-1: Lithostratigraphy	M. Schwarz, P. Schürch, P. Jordan, H. Naef, R. Felber, T. Ibele & F. Casanova
IV	TBO Rheinau-1-1: Microfacies, Bio- and Chemostratigraphic Analysis	S. Wohlwend, H.R. Bläsi, S. Feist-Burkhardt, B. Hostettler, U. Menkveld-Gfeller, V. Dietze & G. Deplazes
V	TBO Rheinau-1-1: Structural Geology	A. Ebert, S. Cioldi, E. Hägerstedt, L. Gregorczyk & F. Casanova
VI	TBO Rheinau-1-1: Wireline Logging and Micro-hydraulic Fracturing	J. Gonus, E. Bailey, J. Desroches & R. Garrard
VII	TBO Rheinau-1-1: Hydraulic Packer Testing	R. Schwarz, M. Willmann, P. Schulte, H. Fisch, S. Reinhardt, L. Schlickenrieder, M. Voß & A. Pechstein
VIII	TBO Rheinau-1-1: Rock Properties and Natural Tracer Profiles	J. Iannotta, F. Eichinger, L. Aschwanden & D. Traber
IX		
X	TBO Rheinau-1-1: Petrophysical Log Analysis	S. Marnat & J.K. Becker
	TBO Rheinau-1-1: Summary Plot	Nagra

1.4 Scope and objectives of this dossier

The dossier at hand describes the results of the stochastic petrophysical log analysis performed in the RHE1-1 borehole. The detailed workflow for this analysis is described in a methodology report (Marnat & Becker 2021). Though the general workflow as described in Marnat & Becker (2021) is still followed, the results documented here also indirectly include information from other boreholes. Interpretation intervals and important parameters have been streamlined between the different boreholes wherever possible. Hence, results should be used for qualitative comparisons with previous work only. The general workflow is only shortly summarized here. Final, comparable results for all boreholes will be documented in a separate report.

The lowest vertical resolution tools, such as ECS, gamma ray or Sonic, are limiting the resolution of the MultiMin analysis. High resolution and standard tools cannot be mixed in the same processing (because the increased number of samples would potentially give the high-resolution logs more weight). For this reason, only the standard resolution version of the logs was input with a sampling rate of ½ foot (~ 15 cm).

For the Multimineral Log Analysis (abbrev. MultiMin throughout this report), a mineral content is assumed at each of these measurement locations from prior knowledge. A theoretical log response from this assumed mineral content for each available petrophysical log is calculated and compared to the measured log. Using optimisation techniques, the difference (i.e. the error) between calculated log responses and measured petrophysical logs is minimised by adjusting the assumed mineral content. Any deviation from this workflow is explained in this report.

The results of this analysis are continuous profiles of the mineralogical content and other rock properties (e.g. porosity) where the main aim of these calculations here were continuous profiles of the clay content and porosity.

The organisation of this dossier follows the necessary steps of the workflow. First, data is collected, and quality checks (QC) are performed. In addition, necessary pre-calculations concerning important environmental parameters are performed (Chapter 2). This is followed by the actual analysis of the data (Chapter 3) and a short description of results in Chapter 4. Chapter 4 also includes an estimation of the fit of the results to available data from lab measurements.

All depths in this report are reported as measured depths from top rig cellar (MD) if not stated otherwise.

2 Data preparation

2.1 Used log data

The acquisition, QC (quality control) and generation of log composites of the petrophysical logs from the borehole RHE1-1 is described in more detail in Dossier VI, the raw corrected log data is also shown in Plate 1. Note that abbreviations in brackets in the list below are according to Schlumberger (SLB) mnemonics (as SLB was the log contractor responsible for the log acquisition). A detailed description of how the different tools measure the respective parameters and the underlying physics behind these measurements is not the focus of this report and can be found in Dossier VI, Chapter 3.1. The petrophysical logs used for this study are listed below:

- **Calliper log** (EMS/PPC – Environmental Measurement Sonde/Powered Positioning Calliper). The calliper log uses several coupled pairs of mechanical arms (2 pairs with PPC, 3 pairs with EMS) to continuously measure the borehole shape in different orientations.
- **Gamma Ray** (ECGR_EDTC, from the EDTC – Enhanced Digital Telemetry Cartridge). This log measures the naturally occurring radioactivity which can be used to determine the mineral content (mainly clay).
- **Spectral Gamma Ray** (SGR, from the HNGS – Hostile Natural Gamma Ray Sonde). This tool also measures the naturally occurring radioactivity. In addition to the total radioactivity, the tool is able to determine the amount (in ppm or wt.-%) of uranium (U), thorium (Th) and potassium (K) in the rocks which can be used e.g. for clay typing.
- **Neutron Hydrogen Index** (APLC curve, from APS – Accelerator Porosity Sonde). The APS is a tool that can measure the neutron hydrogen index in water saturated formations.

  This measurement is corrected for environmental effect and normalised to limestone matrix. SLB refers to this corrected curve as APLC (Near/Array Corrected Limestone Porosity). In addition, the APS can be used to determine **Sigma** (SIGF), a measure to determine the water content and mineralogical characterisations.
- **Density** (TLD – Three-detector Lithology Density). TLD is an induced radiation tool that measures the bulk density of the formation and the photoelectric factor (PEF). It uses a radioactive source to emit gamma photons into the formation. The gamma rays undergo Compton scattering by interacting with the atomic electrons in the formation. Compton scattering reduces the energy of the gamma rays in a stepwise manner and scatters the gamma rays in all directions. When the energy of the gamma rays is less than 0.5 MeV, they can undergo photoelectric absorption by interacting with the atomic electrons. The flux of gamma rays that reach each of the detectors of the TLD is therefore attenuated by the formation, and the amount of attenuation is dependent upon the electronic density of the formation, which is related to its bulk density. In addition, the TLD provides the **photoelectric absorption index** (photoelectric factor – PEF), which represents the probability that a gamma photon will be photo-electrically absorbed per electron of the atoms that compose the material. The PEF characterises the mineralogy. The TLD tool is housed in the High-Resolution Mechanical Sonde that also includes the Micro-Cylindrically Focused Log (MCFL) sonde, that measures the micro-resistivity or alternatively, the resistivity very close to the borehole wall (RXOZ).

- **Element Spectroscopy** (ECS – Elemental Capture Spectroscopy). The ECS is also an induced radiation tool with a radioactive neutron source. The ECS measures the concentration of a series of elements in the formation by analysing the spectrum of back scattered gamma rays. The following elements are used in this report: DWSI_WALK2 (Si), DWCA_WALK2 and DWCA_MGWALK (Ca), DWFE_ALKNA (Fe), DWSU_WALK2 and DWSU_ALKNA (S), DWAL_ALKNA (Al), DWK_ALKNA (K). The curves with MGWALK and ALKNA suffixes are obtained with additional closure models to the standard WALK2. The element spectroscopy measurements are provided in weight concentrations.

  During the QC process of the ECS acquisition, the DWMG_MGWALK response could be validated in the pure dolomites, reading close to the theoretical end-point for dolomites: 0.132 W/W.

  The iron concentration from the ECS ALKNA closure model (DWFE_ALKNA) was preferred to the WALK2, as the results are closer to the XRF core measurements and are in better agreement with the core mineralogy in regional boreholes.

  The same logic applied to the DWSU_ALKNA curve, better correlated to the pyrite concentration (from XRD) in the regional boreholes.

- **Resistivity** (HRLT – High Resolution Laterolog array Tool). The HRLT measures the formation electrical resistivities at different depths of investigation, providing a mud filtrate invasion profile, if any invasion. Processing allows the extrapolation of the resistivity measurements far into the formation (true formation resistivity), as well as close to the borehole wall (micro-resistivity). The resistivity is a function of the water content of the formation and its salinity.

- **Sonic** (MSIP – Modular Sonic Imaging Platform. The MSIP measures the formation interval transit time, a measure of how fast seismic waves (compressional, shear and Stoneley waves) propagate through the formation.

An overview of the used petrophysical logs and their measurements in the borehole RHE1-1 is given in Plate 1.

Usable log data were available for analysis from 35.81 to 824.79 m (USM to Bänkerjoch Formation, see Plate 1). Due to gaps between drilling sections and cased hole sections (see Dossier I), a minor MultiMin interpretation gap, due to insufficient petrophysical logs coverage, remained in the following interval, as shown in Fig. 2-1:

- 494.7 – 497.4 m (Bottom ½" Section I at 497 m MD driller's depth, 7⅝" casing shoe at 496 m MD driller's depth)

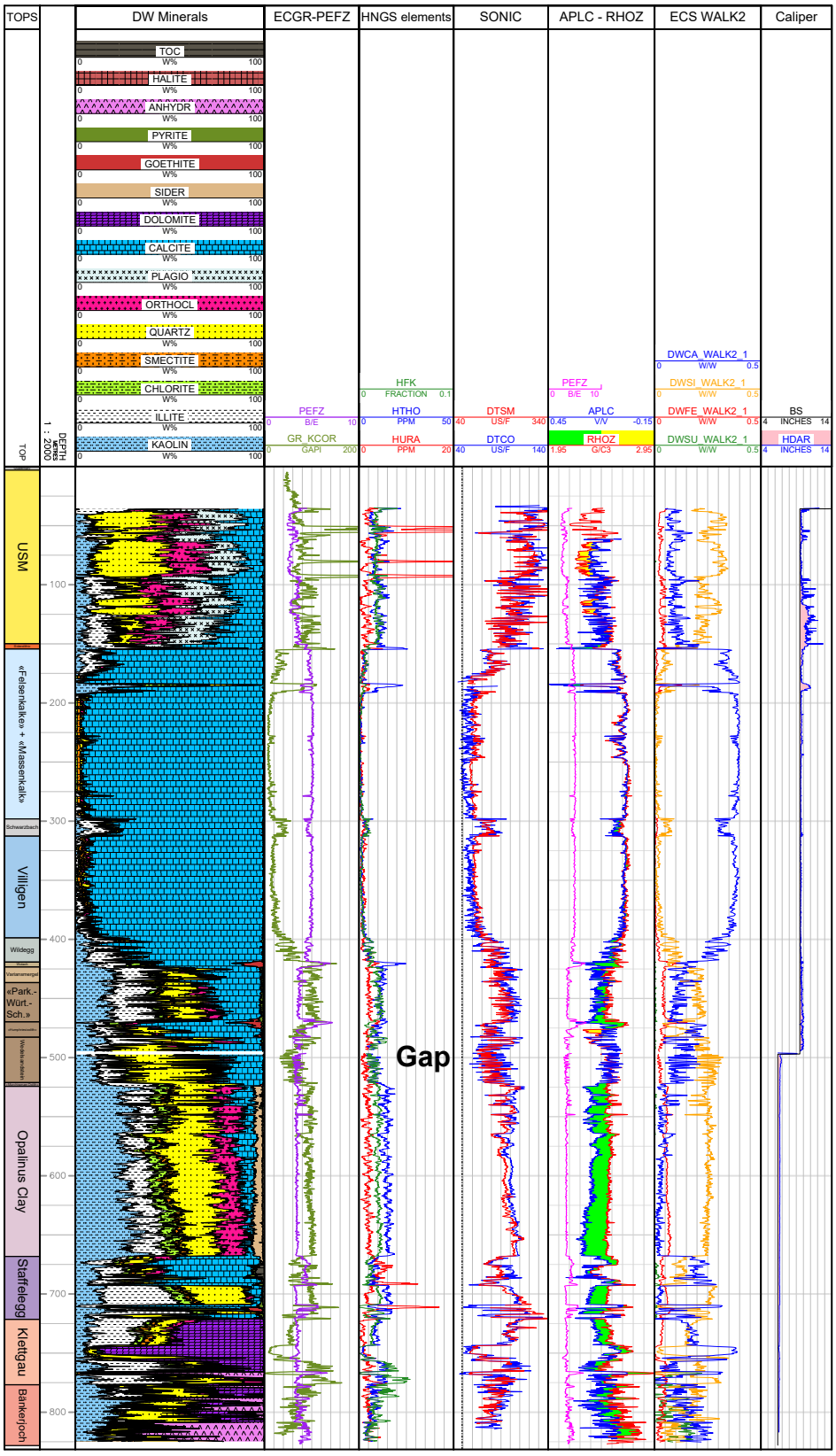

Fig. 2-1: Petrophysical log availability and gaps in the RHE1-1 borehole

Please note that ECS elements are displayed as measured (in weight/weight, 0 – 1 w/w range) and are not converted to wt.-% (weight percentage) here.

2.2 Used core data

As previously mentioned, no laboratory measurements were performed in RHE1-1.

Nevertheless, core mineralogical measurements from four reference boreholes (MAR1-1, BOZ1-1, BOZ2-1 and TRU1-1) are implicitly used in this study to compute three accessory minerals: TOC, smectite and chlorites. A Multi-Resolution Graph-Based Clustering (MRGC, see Ye & Rabiller 2000) was run to predict these three minerals' volumes.

The training dataset was built for each predicted mineral from wireline log data (ECS elements, HNGS elements, Neutron Hydrogen Index, SIGF, Bulk Density and PEFZ) and an associated log from core data (TOC, smectite or chlorites, wt.-%). The MRGC algorithm is classifying this training dataset into several clusters. Then, the associated log can be predicted as the average of the K Nearest Neighbours (KNN, 5 nearest neighbours). The resulting curves for TOC, smectite and chlorites were then used, with a high weight (see Marnat & Becker 2021), as an input for the MultiMin interpretation.

2.3 Multi-sensor core logger data (MSCL)

MSCL measurements from cores were available in the borehole RHE1-1 (from 499.15 to 827.75 m driller's depth). Measurements were performed in the interval of the host rock (Opalinus Clay) and its confining units. The following parameters were measured:

- Bulk density in g/cc
- Compressional (P) wave velocity in m/s
- Spectral gamma ray curves: potassium (K, %), thorium (Th, ppm) and uranium (U, ppm)
- XRF (X-ray fluorescence) elemental analysis.

Some ECS data could not be acquired between drilling sections, leaving a gap. In these same intervals, no or limited XRF data is available to fill the gaps.

The XRF elemental analysis results were compared with the same elements' concentration from the ECS logging (WALK2 closure model). The MSCL data (also referred to as core logs in this report) covers the measured interval at variable sampling rates (usually 0.05 m).

This comparison is shown in Fig. 2-2 for RHE1-1, the core logs were depth-shifted using the Core Goniometry depth shift table.

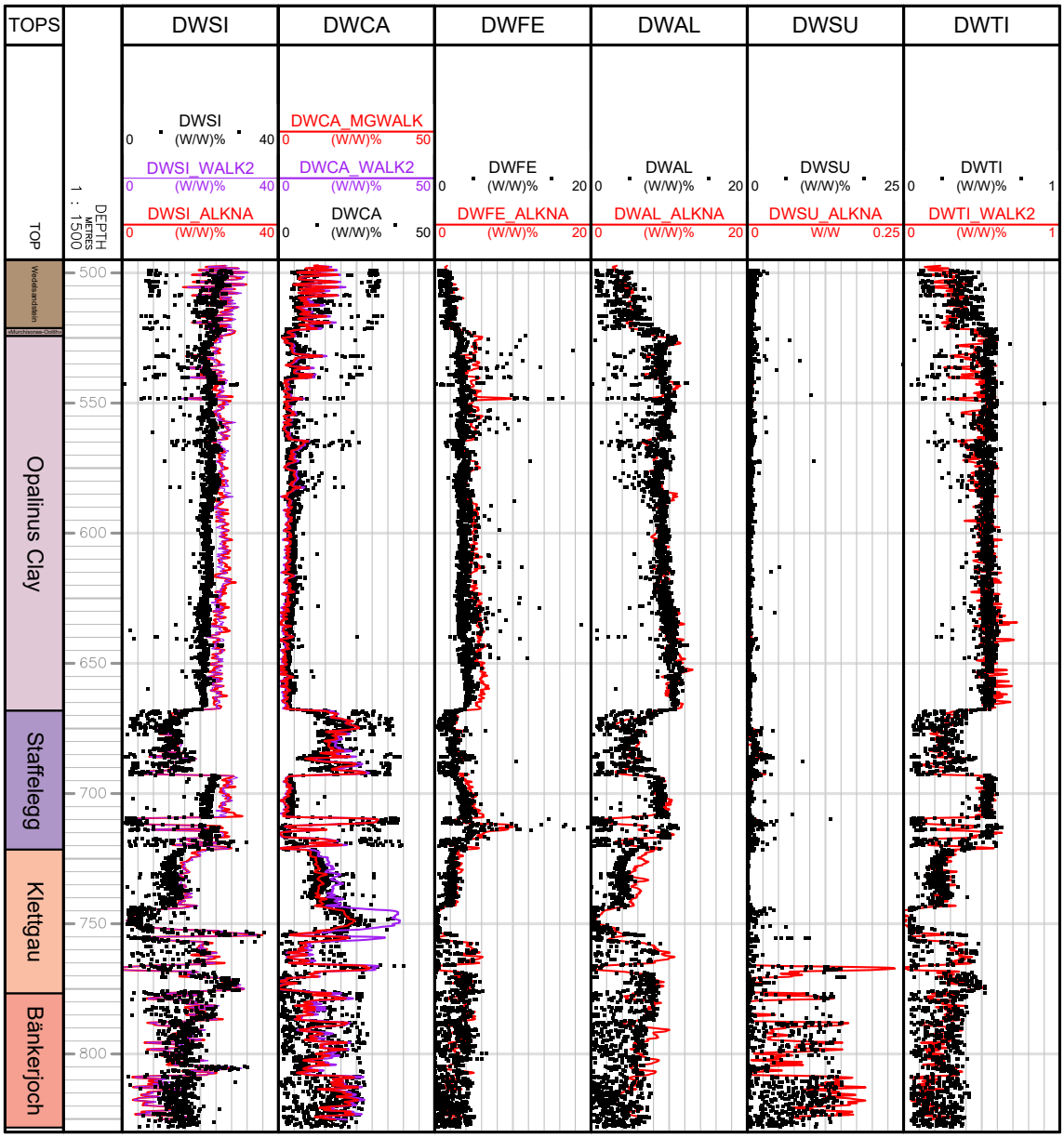

Fig. 2-2: XRF (black dots) and ECS (red and purple curves) elements comparison in RHE1-1

While the calcium, aluminium (from the ALKNA closure model) and titanium concentrations are almost similar, the XRF iron and silicon are slightly lower than ECS.

The same check was done for the core, ECS and HNGS spectral gamma ray (see Fig. 2-3).

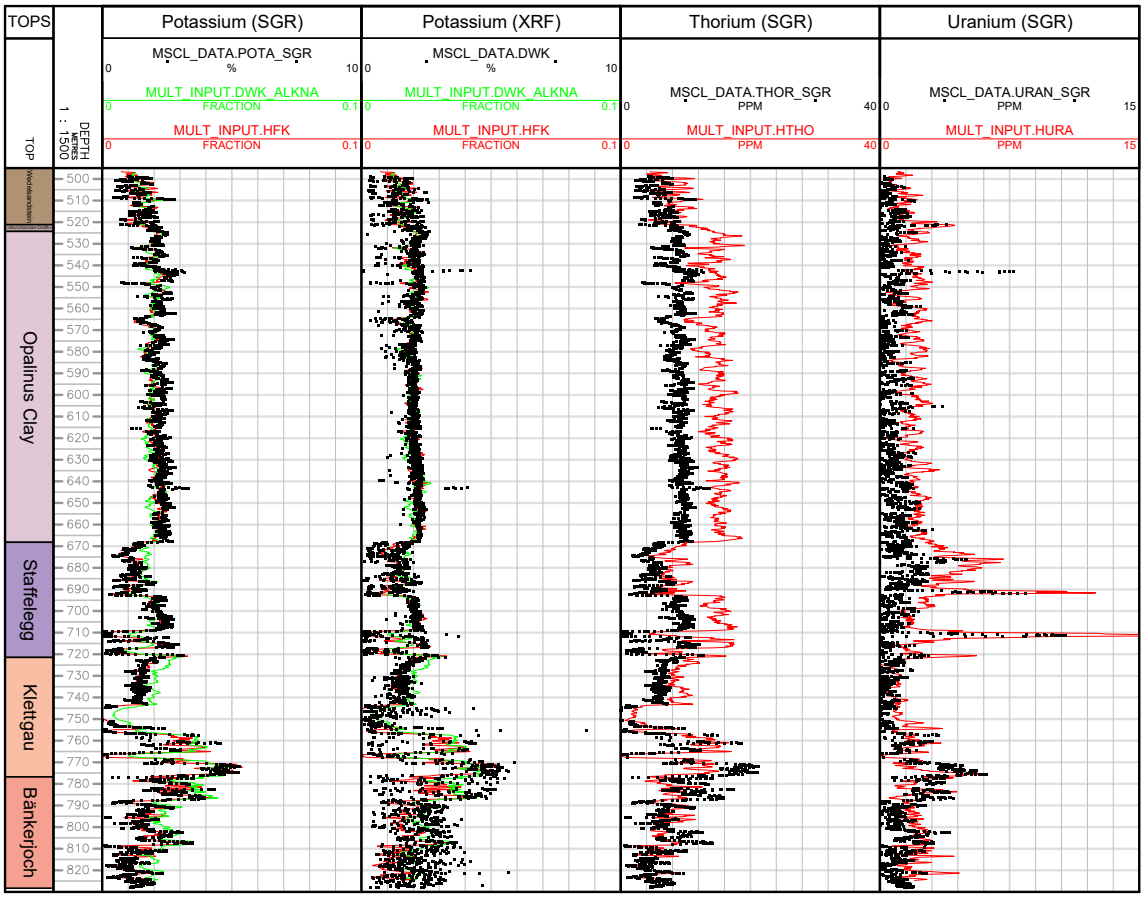

Fig. 2-3: Core (black dots: spectral gamma ray, and XRF potassium) and wireline (red curves for HNGS, green curve ECS potassium) spectral gamma ray elements comparison

The potassium content from MSCL and wireline logs (ECS, HNGS) is similar.

The HNGS thorium and uranium are higher than the MSCL spectral GR curves.

Hence, the MSCL data was used indirectly for the QC of the ECS and HNGS measurements.

2.4 MultiMin input dataset preparation

The petrophysical composite log used as input for this study (see Dossier VI) represents a quality controlled, edited, corrected and merged dataset for a selection of the most important petrophysical logging data recorded in each section of the borehole. As mentioned earlier, a gap in the coverage of the borehole with petrophysical logs occurs. The original measurements and corrections of the petrophysical logs are reported in Dossier VI.

At the bottom of the 9½" hole section, the HNGS was not acquired below 493.2 m. As the ECS was run below this depth with the ALKNA closure model, the ECS potassium curve DWK_ALKNA was used instead. This curve was cross-plotted against HFK in the same hole section, and was corrected to HFK, as shown in Fig. 2-4 here after.

The HFK_DWK curve was generated as follows:

HFK_DWK (%) = 110.867 * DWK_ALKNA (W/W) – 0.312127

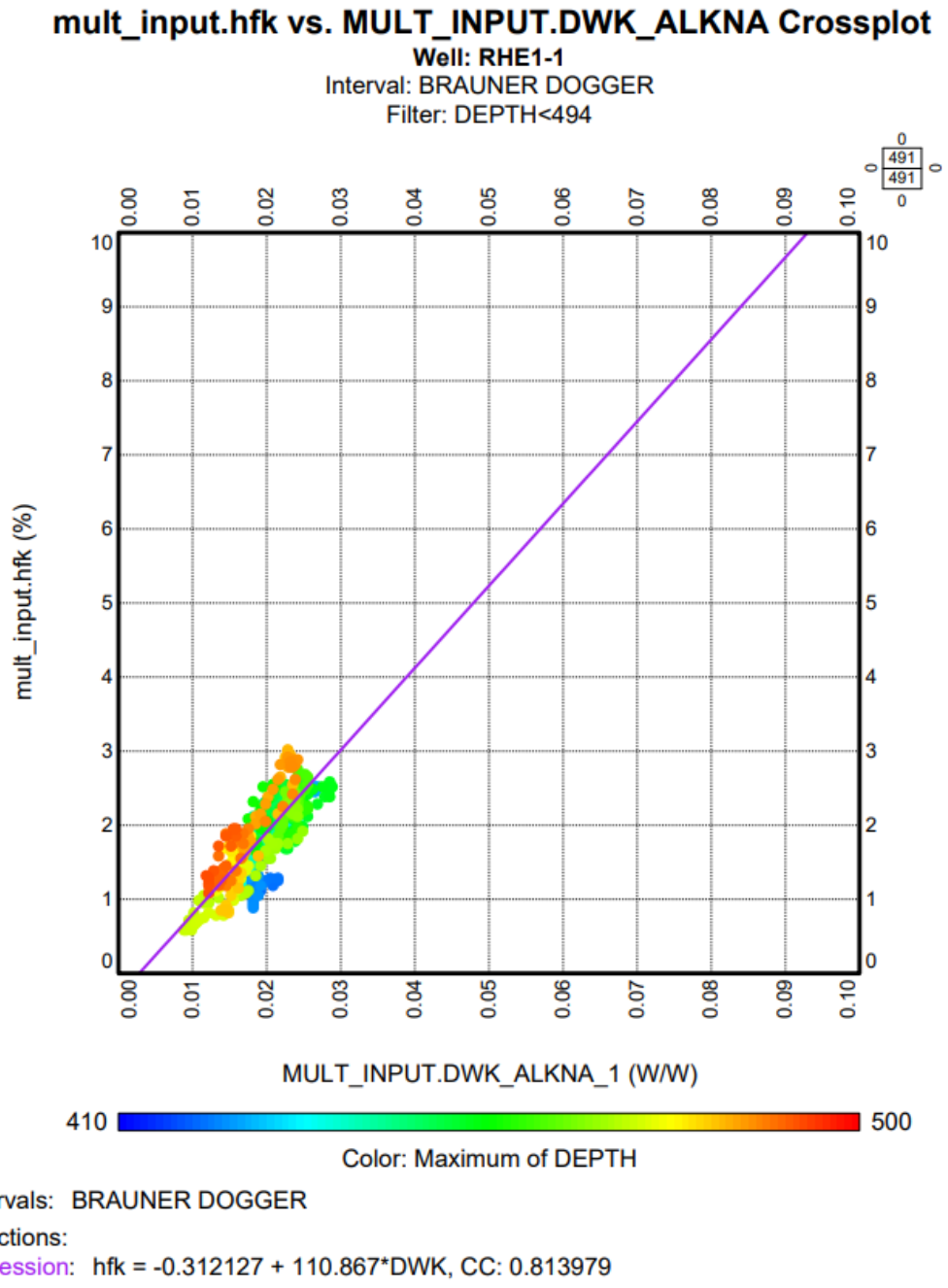

Fig. 2-4: HFK versus DWK_ALKNA in the 9½" hole section

2.5 Preliminary calculations (Precalc)

As the wireline logs measure parameters under in situ conditions (e.g. temperatures depending on depth and temperature of the borehole fluid, infiltration of mud into the formation depending on the borehole fluid and its density etc.), these prevailing conditions in the borehole have to be taken into account to correctly predict/calculate the theoretical log response from the assumed mineral and fluid content (i.e. total porosity) at a certain depth. Continuous profiles of these environmental parameters were calculated using the Precalc module from the interpretation software Geolog. The main parameters used for the calculation of these environmental parameters are, for reasons of transparency and to be able to replicate exactly the analyses reported here, displayed in Appendix A.

The mud properties (mud density and resistivities) reported here were extracted from the validated SLB wireline log headers (see Dossier VI).

3 Petrophysical log interpretation

3.1 MultiMin interpretation

In the following, the petrophysical log interpretation and its results are shortly described. All necessary data treatment and environmental pre-calculations have been described in the previous chapters or are described in the Methodology report (Marnat & Becker 2021).

Many qualitatively good wireline logs were available in most of the borehole, allowing the computation of many unknowns (fluids and minerals).

Significant hydrocarbon shows were neither described by the mudlogging nor inferred from cores or petrophysical logs. Consequently, the formations were treated as water wet (i.e. with saline water as the pore fluid).

The main minerals were inferred from the XRD measurements on core samples from recently drilled boreholes (BUL1-1, TRU1-1, MAR1-1, BOZ1-1, BOZ2-1, STA2-1, STA3-1 and BAC1-1, see Dossiers VIII of the respective borehole reports), Weiach-1 and Benken-1 from Mazurek (2017). Using the MultiMin approach, the mineral content for the following minerals were modelled:

- Clay mineral endmembers (kaolinite, illite, smectite and chlorites), non-potassic clays and total clay mineral content
- Silicates: quartz, potassic feldspars, plagioclases
- Carbonates: calcite, siderite, dolomite/ankerite
- Iron-rich minerals: goethite, pyrite
- Evaporites: anhydrite
- Organic carbon (kerogen, quantified by TOC)

These compounds were modelled depending on the available data. In case not enough data were available for a given interval (e.g. where data was missing or of insufficient quality), some minerals were merged to a pseudo-mineral to reduce the number of unknowns (see Marnat & Becker 2021 for more details).

Tab. 3-1 shows the interpretation intervals in RHE1-1 and the MultiMin model names used in each interval. The intervals are defined based on their consistent mineralogy, available logs and consistent environmental parameters (e.g. mud system changes). Interpretation intervals may be subdivided further, e.g. to respect a reduced data quality. The full table with all intervals is available in Appendix B.

Mineral and fluid endpoints were manually optimised to both reduce the difference between measured and predicted logs and match the core mineralogy and porosity. Greatly simplified, an endpoint can be regarded as a factor that is used to calculate the theoretical log response for each mineral (e.g. if it is assumed that the endpoint for the density of calcite is 2.71 g/cc, a mineral content of 100% calcite should result in a density of 2.71 g/cc of the predicted density log; for a detailed explanation see Marnat & Becker 2021).

Tab. 3-1: List of MultiMin models used in RHE1-1

The intervals (column Interval name) may include several MultiMin models if some of the input data were of bad quality or the particular section of the interval required special assumptions due to its assumed mineralogy.

The column Cond Num stands for model condition number. Low values are typical for good mathematical models (below 4.00; highlighted in green). Condition numbers above 4.00 highlighted in orange correspond to fair models. See Section 3.2 for more information.

From (m)	To (m)	Interval name	Multimin Models	Cond Num	Description
35.3	61.3	USM	rhe11_usm_noaps	3.60	APS not available
61.3	67.4	USM	rhe11_usm_gh	2.99	Good hole conditions
67.4	68.3	USM	rhe11_usm_nodt	2.99	DTCO gap
68.3	154.5	USM-Siderolithic	rhe11_usm_gh	2.99	Good hole conditions
154.5	182.4	MALM	00_malm_al_rev	4.09	Using ALKNA closure model
182.4	183.7	MALM	00_malm_rhe11_nodt	4.12	DTCO gap
183.7	186.5	MALM	00_malm_rhe_top	3.50	Facies change (karst?)
186.5	189.1	MALM	00_malm_al_rev	4.09	Using ALKNA closure model
189.1	192.0	MALM	00_malm_rhe_top	3.50	Facies change (karst?)
192.0	418.6	MALM	00_malm_al_rev	4.09	Using ALKNA closure model
418.6	476.0	BRAUNER DOGGER	00_bd_rhe1	3.94	Model with goethite
476.0	479.7	BRAUNER DOGGER	00_bd_bh_rhe	3.93	Density affected by hole conditions
479.7	489.6	BRAUNER DOGGER	00_bd_rhe1	3.94	Model with goethite
489.6	493.2	BRAUNER DOGGER	00_bd_noct_rhe	3.96	HRLT missing at section bottom
493.2	494.8	BRAUNER DOGGER	00_bd_notld	4.12	TLD missing at section bottom
494.8	497.4		Gap		Not enough logs
497.4	497.7	BRAUNER DOGGER	00_bd_noct_rhe	3.96	HRLT missing at section top
497.7	524.2	BRAUNER DOGGER	00_bd_rhe1	3.94	Model with goethite
524.2	692.4	OPA - STAFFELEGG	opa_sta_rhe	3.51	Opalinus & top Staffelegg
692.4	711.3	STAFFELEGG	sta	3.74	Staffelegg
711.3	715.0	STAFFELEGG	00_sta_goeth_rhe11	3.93	Model with goethite
715.0	721.2	STAFFELEGG	sta	3.74	Staffelegg
721.2	756.1	KLETTGAU	klet_rhe	3.56	Top Klettgau, Mg from ECS
756.1	776.6	KLETTGAU	klet_base_al	3.69	Base Klettgau, high HFK
776.6	814.0	BSZ (*)	00_bsz_mg_al	3.72	Bänkerjoch, ALKNA&MGWALK
814.0	822.6	BSZ (*)	00_bsz_noctdt	3.93	No DTCO & HRLT at section bottom
822.6	824.9	BSZ (*)	00_bsz_noaps	4.08	No APS at section bottom
824.9	825.3	BSZ (*)	Gap		Not enough logs

BSZ (*): Bänkerjoch, Schinznach, Zeglingen

Based on expert judgement, an uncertainty value for the petrophysical logs was estimated and used to adjust the weight given to the respective log in the MultiMin computation. Again greatly simplified, if the uncertainty values are large, the corresponding log response will be predicted in the MultiMin interpretation, but it will not be used in the process of error minimisation and hence has no impact on the result of the MultiMin interpretation (for more details see Marnat & Becker 2021). High uncertainty values often apply to the Sonic, the Total GR and the electrical conductivities.

The detailed parameters for all the MultiMin models are available in tables in Appendix C.

3.2 Bad hole treatment and quality of results

The quality of the MultiMin interpretation relies in part on the quality of the input data. However, it also relies on the number of available curves and the number of unknowns (i.e. minerals) that need to be calculated. Hence, several quality indicators exist that either are informative about the quality of the input data (LQC-Index), the definition of the mathematical model (CONDNUM, NFUN) or the quality of the interpretation results (MULT_QC and QUALITY).

3.2.1 Indicator for input data quality (LQC_INDEX)

During each wireline logging, the borehole shape is determined using a caliper log. If the borehole shape deteriorates far from the bit size (BS) and bit shape (usually circular), some (or all) of the wireline logs may measure biased data, because the distance between the log and the borehole wall is too large. In that case, the response of a considerable amount of borehole fluid is measured by the tool and the measurements represent more the petrophysical parameters of the borehole fluid than of the formation.

Four bad hole indicators, which can be used as a quality measure of the data, are calculated from some of the available wireline logs:

1. FLAG_ND: Neutron-Density crossplot, flagging bad hole from expert picking in the density-neutron crossplot. It is shown in Fig. 3-1
2. FLAG_BADHOLE_OVERGAUGE: HDAR > 1.15 * Bit Size
3. FLAG_BADHOLE_RUGO: Borehole wall rugosity, HDRA > 0.025 g/cc: HDRA (bulk density correction) is a correction of the bulk density measured with a gamma-gamma type logging device (here TLD). If this correction factor is larger than 0.025 g/cc, the indicator is triggered
4. FLAG_BADHOLE_STOF: APS Neutron standoff > 0.35 in

For detailed information about these four indicators, please refer to Dossier VI.

These four indicators have two possible values: 0 in good hole or 1 in bad hole. They were combined to generate a log quality control flag (LQC_INDEX) using the following equation:

LQC_INDEX = (FLAG_BADHOLE_DN + FLAG_BADHOLE_OVERGAUGE +

FLAG_BADHOLE_RUGO + FLAG_BADHOLE_STOF) / 4

Hence, the value of the LQC-Index must be between 0 and 1 (and can only have values of 0, 0.25, 0.5, 0.75 or 1).

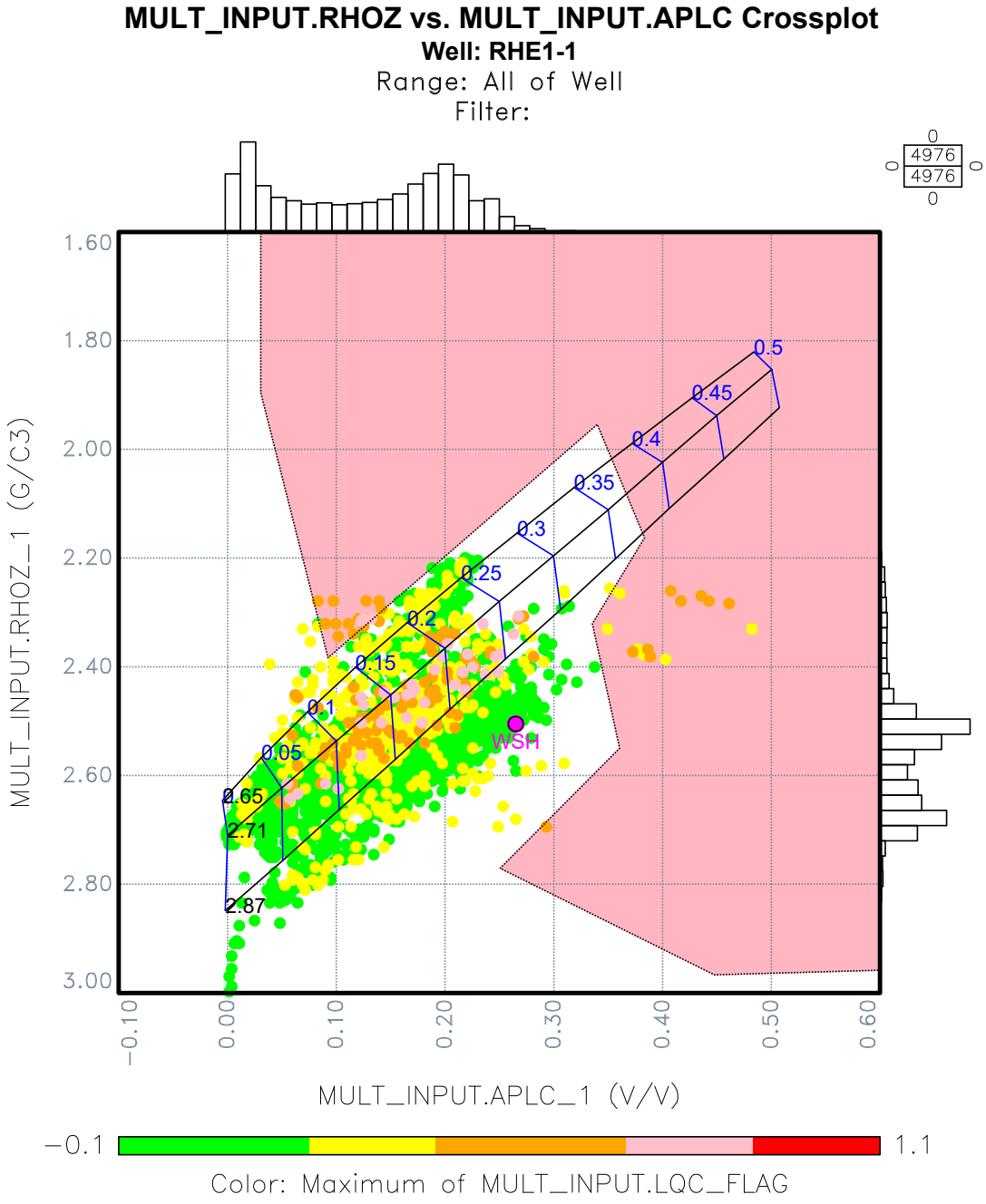

Functions:
SB_APLC_Phi_fw: Porosity from Formation Density & APLC (RHO_FL = 1.00 g/cc)
SB_APLC_rho_fw: RHO_MAA from Formation Density & APLC (RHO_FL = 1.0 g/cc)
dn_bh: No description given.

Fig. 3-1: Density-Neutron crossplot badhole indicator

The points displayed in the pink shading are flagged.

3.2.2 Indicator for the mathematical model (CONDNUM and NFUN)

CONDNUM

The CONDNUM stands for model condition number. Low values are typical for good mathematical models (below 4.00). Condition numbers above 4.00 correspond to fair models. A list of CONDNUMs for the different MultiMin interpretation intervals is given in Tab. 3-1. Please note that CONDNUM is not a proxy for the quality of the calculated output but only for the definition of the mathematical model to calculate the said output.

NFUN

NFUN indicates how many iterations were required to fulfil the constraints imposed by the available data where fewer numbers of iterations are indicative for a more robust model. NFUN is also shown in Plate 1. Please note that NFUN, as CONDNUM, is not a proxy for the quality of the calculated output but only for the definition of the mathematical model to calculate the said output.

3.2.3 Indicator for the MultiMin interpretation results (MULT_QC and QUALITY)

MULT_QC

The MultiMin results were not edited in RHE1-1 (e.g. less reliable data were not removed from the interpretation results), but an integrative MultiMin QC flag was generated (MULT_QC) combining several of the aforementioned quality indicators to inform the data user of potentially invalid results. The MULT_QC flag relies on expert judgement and can have values of 2, 1 or 0 based on the three different scenarios detailed below:

- Highly suspicious porosity spikes occur and usually are correlated to an LQC-Index above or equal to 0.5, the quality curve (displayed in Plates 1 and 2, see below) can show values above 2: MULT_QC = 2. A value of 2 in MULT_QC corresponds to most likely unreliable data.
- Suspicious porosity spikes occur but with a usually acceptable LQC_Index (0 or 0.25) and MultiMin quality curve values below 2: MULT_QC = 1. This value indicates that results can/should be used for the characterisation of the formation but should be treated with caution as the interpreted results are not a perfect fit with the available data.
- Otherwise, MULT_QC = 0. Interpreted results are reliable and can be used to characterise the formation.

QUALITY

In addition, a quality curve is shown in Plates 1 and 2. This curve is an indication of how well the observed measurements from wireline logs and the predicted results are part of the same population. At a value of QUALITY less than one, the calculated accuracy is within 95% compared to the original wireline logs and therefore the analysis is of good quality. If the value is consistently above one, log measurements are not well honoured by the predicted curves, hence the analysis must be regarded as less robust.

Please note that the quality curve only compares the results of the MultiMin interpretation with the petrophysical logs and does not take data quality of the petrophysical logs (e.g. in bad hole sections) into account. The only indicator combining information on input data quality and interpretation result is the MULT_QC indictor detailed above.

4 Results of the calibrated stochastic log interpretation

In the following, the main results of the stochastic log interpretation are summarised. Plate 1 shows the measured wireline logs together with the calculated output from the MultiMin approach. The main results in terms of mineral content and porosity are displayed in Plate 2 as continuous curves.

The aim of this chapter is not a detailed description and characterisation of the sedimentary sequence based on log interpretation results, but rather gives a more general description of the data and a general characterisation of the stratigraphic system or groups shown in Plate 2. Section 4.1 gives a general characterisation while Section 4.2 gives a more detailed description of calculated parameters in the Opalinus Clay.

4.1 Main results of the log analyses in the borehole RHE1-1

The main aim of the MultiMin interpretation were continuous curves of porosity and clay content of the borehole RHE1-1. Several other minerals have been determined (mainly QF-silicates and carbonates). Below is a summary of the main parameters of clay, carbonate, QF-silicate content and porosity for each system/group.

If not stated otherwise, clay content is used senso lato meaning that clay content is used as a general term for the total clay mineral content of the formation (i.e. the sum of all clay minerals). Carbonates and QF-silicates are also used sensu lato where carbonates are regarded as the sum of all carbonate minerals (calcite, dolomite and siderite) while QF-silicates is used synonymously for the sum of quartz (senso stricto) and feldspars.

USM (3 – 149.9 m) and Siderolithic (149.9 – 154.4 m)

The top part of the USM was not logged down to 35.8 m. The LQC_FLAG shows good hole down to 95 m, then small washouts and rugosity below, although the logs seem to remain unaffected.

As the logs response (mostly the Density-Neutron separation) suggests a light matrix and core data from other boreholes with comparable lithology show a large amount of potassic feldspars and plagioclases in the USM formation, plagioclases were added to the MultiMin model.

The major matrix minerals are quartz (mean of 24.0 wt.-%, median 25.3 wt.-%), potassic feldspars (mean of 17.0 wt.-%, median 17.2 wt.-%), plagioclases (mean of 22.3 wt.-%, median 22.5 wt.-%), and calcite (mean of 20.2 wt.-%, median 19.1 wt.-%).

The clay content generally remains below 30 wt.-% (except in the rat hole at the top section), with a mean of 16.0 wt.-%, and a median of 14.9 wt.-%. The clay typing remains uncertain in the USM, as it cannot be checked against core measurements.

Malm (154.4 – 419.2 m, «Felsenkalke» + «Massenkalk», Schwarzbach Formation, Villigen Formation and Wildegg Formation)

As expected, calcite is the main constituent in the formations of the Malm, the mean calcite content is 88.9 wt.-% (median of 92.3 wt.-%). Lithological changes (e.g. at group boundaries) are sometimes reflected in a sharp negative peak (i.e. decreasing carbonate content at top Schwarzbach Formation correlated to clay content increase), but in general variance of the carbonates in the Malm is low.

Only the Schwarzbach and Wildegg Formations are more argillaceous and correlatively less calcareous: respectively mean / median 16.3 / 17.3 wt.-% clays and mean / median 79.4 / 78.5 wt.-% calcite in the Schwarzbach Formation and mean / median 22.8 / 23.4% clays and mean / median 71.9 / 71.5 wt.-% calcite in the Wildegg Formation.

The QF-silicate content in the Malm is low (mean of 2.7 wt.-%, median of 2.1 wt.-%). The more clay-rich lithologies (Schwarzbach Formation and Wildegg Formation) show a slightly increased QF-silicate content (mean / median of the Schwarzbach Formation: 3.5 / 3.4 wt.-%, Wildegg Formation: 4.3 / 3.7 wt.-%).

Total porosity in the Malm ranges between 0 and 11.7% (mean of 2.9%, median of 2.2%). The highest porosities are observed in the Schwarzbach Formation but may be slightly overestimated as they might represent artefacts due to a reduced data quality in these intervals.

A different lithology is observed in the interval 183 to 192 m: high GR, high APLC and SIGF, low density, high iron content at top. This may represent siderolithic filling in a cave.

Dogger (419.2 – 668.19 m, Wutach Formation, Variansmergel Formation, «Parkinsoni-Württembergica-Schichten», «Humphriesioolith Formation», Wedelsandstein Formation, «Murchisonae-Oolith Formation», Opalinus Clay)

The boundary between the Malm and the Dogger is clearly marked by a sharp increase of the iron content (up to 16.8 wt.-%) and the thorium content, and a sharp decrease of the carbonate content to the Wutach Formation. In the regional boreholes, these changes are correlated with a high goethite content (high Fe and adsorbed Th).

The carbonate content in the Dogger is generally moderate, with a mean of 20.5 wt.-% and a median of 15.2 wt.-% (maximum 68.2 wt.-% in the «Humphriesoolith Formation»). The carbonate content is dominated by calcite above the Opalinus Clay (mean / median 31.6 wt.-% / 28.9 wt.-%), and calcite plus siderite in the Opalinus Clay (mean / median calcite 8.1 wt.-% / 6.9 wt.-%; mean / median siderite 4.4 wt.-%).

Several calcite-rich thin streaks can be noticed in the upmost half of the Opalinus Clay, visible on the bulk density RHOZ and the calcium content DWCA_WALK2. These streaks are likely not well characterised due to the limited vertical resolution of the ECS tool.

The QF-silicate content in the Dogger ranges between 1.5 and 55.8 wt.-%. The mean and median values (32.5 and 34.3 wt.-%) are heavily influenced (increased) by the Wedelsandstein Formation (mean / median 40.8 / 41.1 wt.-%) and the thin «Murchisonae-Oolith Formation», while the other formations are in the range between 1.5 and 44.9 wt.-%.

The Opalinus Clay in the Dogger certainly is the formation with the highest clay content, ranging between 29.2 and 66.8 wt.-% (mean / median of 50.6 / 51.0 wt.-%). The clay content is high but variable in the formations above (minimum 14.0 wt.-%, maximum 63.9 wt.-%, mean / median of 38.1 / 38.5 wt.-%).

Total porosity of the Dogger also is contrasted between the different units. PHIT is not very variable in the Opalinus Clay (minimum / maximum 6.5 / 15.2%, mean / median 10.9 / 10.8% with a low standard deviation of 1.45%). It is more variable in the overlying Dogger formations (minimum / maximum 4.0 / 20.0%, mean / median 10.4 / 10.9% and a standard deviation of 2.9%). This maximum computed value of 20.0% is located within the iron-rich Wutach Formation, analogues were observed in core data in regional boreholes.

Lias (668.19 – 721.5 m, Staffelegg Formation)

The formation boundary from the Opalinus Clay (Dogger) to the Staffelegg Formation (Lias) corresponds to a sharp drop of the clay content and a sharp rise of the carbonate (mostly calcite) content.

The carbonate content of the Lias reflects the lithology where Gross Wolf down to Grünschholz and Beggingen Members have a relatively high carbonate content (mean / median 51.1 / 49.8 wt.-%, up to 81.7 wt.-%), while the Frick and Schambelen Members have a lower carbonate content (mean / median 11.1 / 6.7 wt.-%). As in the previous groups, the carbonate content is dominated by calcite, no significant dolomite content has been measured from cores in the nearby boreholes.

The QF-silicate content shows the reverse of the carbonate content. While the Gross Wolf down to Grünschholz and Beggingen Members show a relatively low QF-silicate content (mean / median 14.1 / 13.9 wt.-%), the lower part (Frick and Schambelen Members) shows higher QF-silicate contents (mean / median 30.0 / 30.1 wt.-%).

The clay content follows the same trend, moderate in the Gross Wolf down to Grünschholz and Beggingen Members (mean / median 30.5 / 30.9 wt.-%) and high in the Frick and Schambelen Members (mean / median 57.0 / 60.8 wt.-%).

The Staffelegg Formation is also characterised by high total organic carbon (TOC), computed using a Facimage prediction (training dataset: MAR1-1, BOZ2-1, BOZ1-1and TRU1-1 boreholes). The maximum computed TOC was 6.4 wt.-% at 686.4 m.

The total porosity in the Staffelegg Formation ranges between 2.6 and 19.6%, the highest values in the Schabelen Member in high clay-content rocks. The total porosity increases with the clay content.

The mean / median PHIT in the Staffelegg Formation is 9.7 / 10.3%.

Keuper (721.5 – 828.24 m, TD, Klettgau Formation, Bänkerjoch Formation)

In the Keuper, the top part of the Klettgau Formation (Gruhalde and Seebi Members) is characterised by a complex mineralogical mixture of carbonates (mostly dolomite) between 0 and 90.8 wt.-% (the latter represents dolomites within the Seebi Member), silicates (quartz and feldspars) between 0 and 63.2 wt.-% and clays (dominant illite) between 2.6 and 83.8 wt.-%. A sandier layer is observed towards the base of the Seebi Member, up to 63.2 wt.-% QF-silicates.

The Gansingen Member is an anhydrite bed, while the base Klettgau Formation (Ergolz Member) is an argillaceous formation (17.5 wt.-% to 69.5 wt.-% clays, mean / median 51.1 / 53.5 wt.-%) with QF-silicates (10.7 wt.-% to 48.2 wt.-%, mean / median 29.6 / 30.8 wt.-%).

The underlying Bänkerjoch Formation is dominated by anhydritic deposits: 0 to 80.4 wt.-% (mean 29.4 wt.-%). In complement, carbonates (dolomite), clays and QF-silicates are well represented in this formation.

The total porosity ranges from 0 to 18.7% (mean 11.2% and median 11.5%). The lowest porosities correspond to the anhydrites (Gansingen Member).

The wireline log quality is good in the Keuper, except at borehole bottom (822 m downwards) where HDRA above 0 g/cc suggests local wall rugosity.

4.2 Main results of the core-calibrated log analysis in the Opalinus Clay (524.33 – 668.19 m)

The main results in terms of total clay content, mineralogy and total porosity for the main focus interval (Opalinus Clay) are shortly described in this section. Figs. 4-1 to 4-8 show some general statistical values of the MultiMin analysis results within the Opalinus Clay.

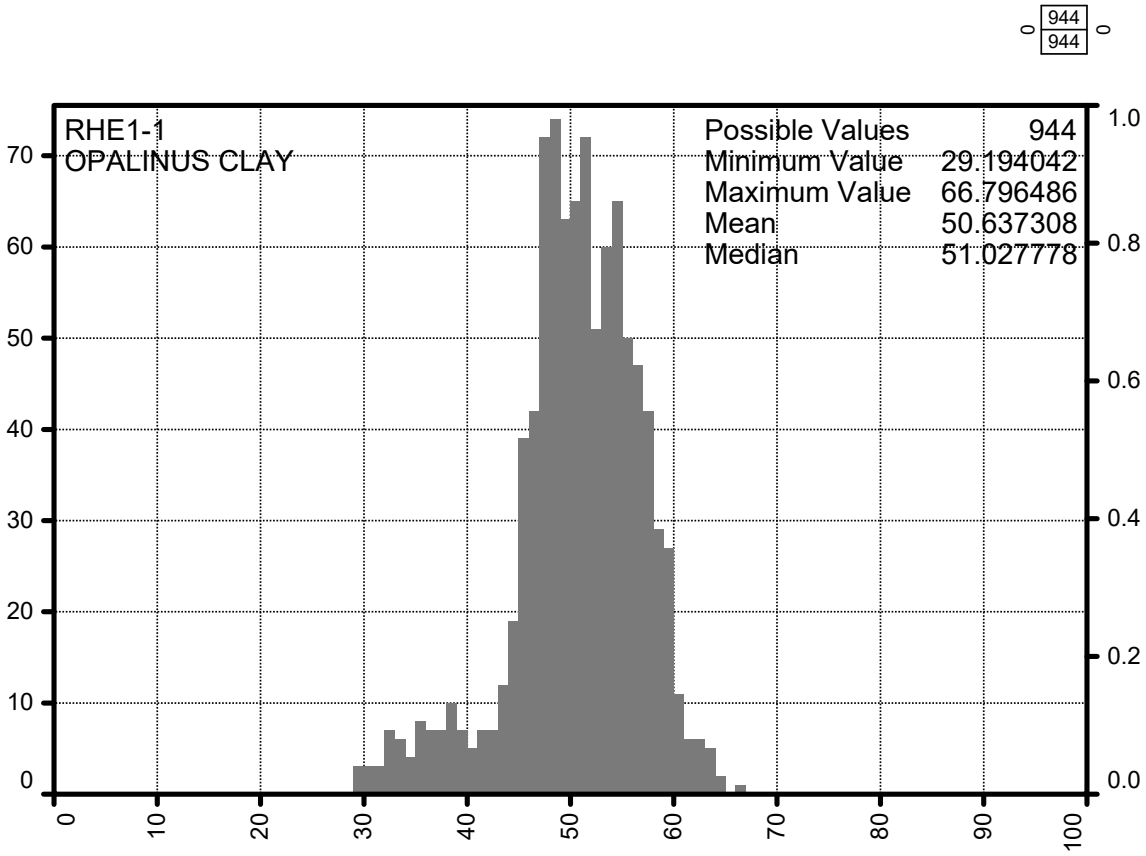

Fig. 4-1: Dry clay weight-percentage frequency histogram in the Opalinus Clay

X-axis is the dry clay wt.-% from MultiMin, y-axis the number of points per bin (100 bins).

In the clay-rich Opalinus Clay, the mean and median dry clay contents are close to respectively 50.6 and 51.0 wt.-%. The lowest clay contents are located in the shallowest part of the Opalinus Clay). The two next frequency histograms show a split of the Opalinus Clay into an upper and lower part, showing that the latter is slightly more argillaceous.

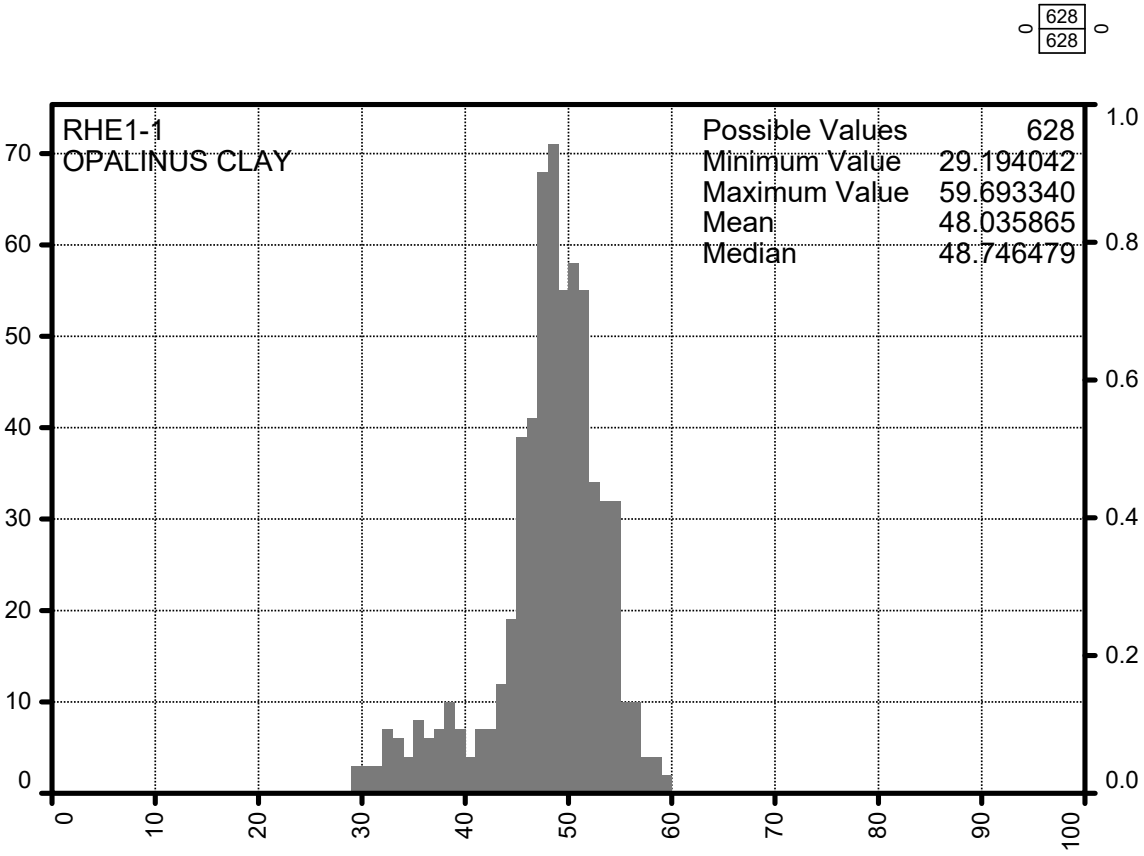

Fig. 4-2: Dry clay weight-percentage frequency histogram in the upper section of the Opalinus Clay (above 620 m)

X-axis is the dry clay wt.-% from MultiMin, y-axis the number of points per bin (100 bins).

In the upper part of the Opalinus Clay (above 659 m), the mean and median dry clay content are close to 48.0 and 48.7 wt.-%. The top part of the formation is less argillaceous than the bottom, see Fig. 4-3.

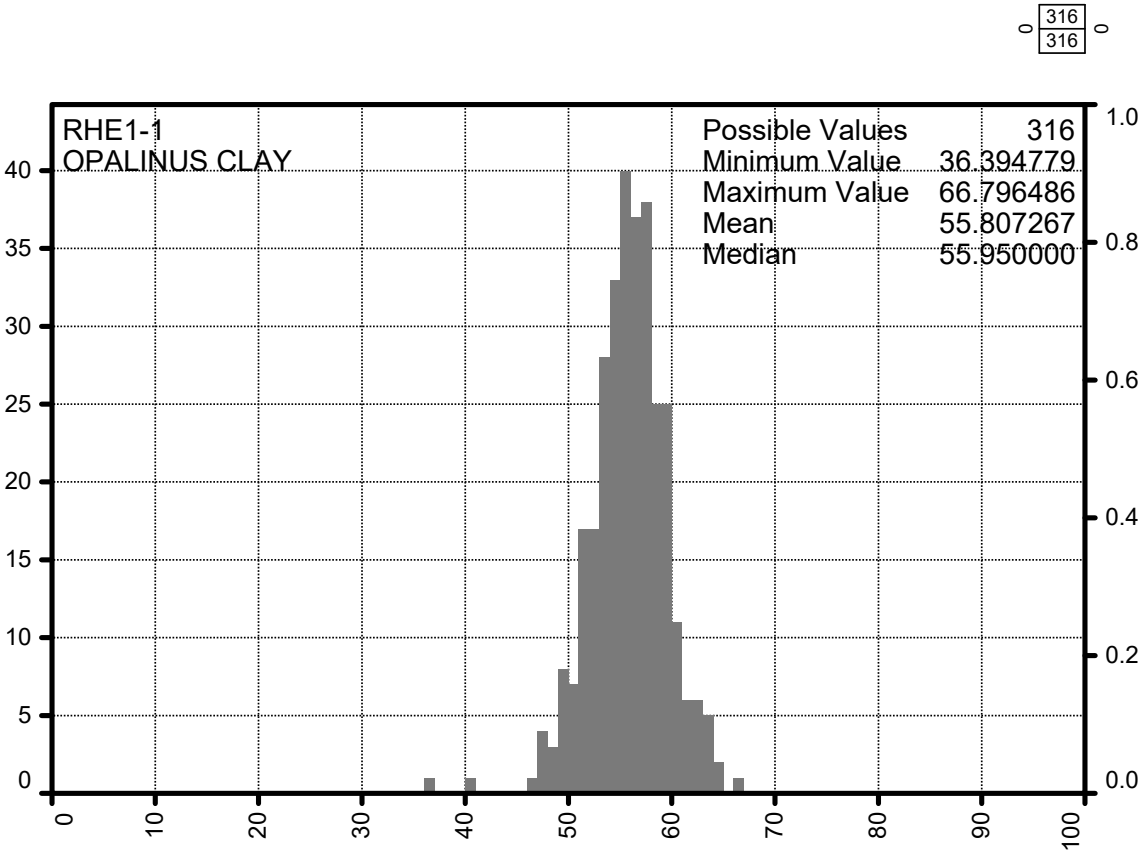

Fig. 4-3: Dry clay weight-percentage frequency histogram in the lower section of the Opalinus Clay (below 620 m)

X-axis is the dry clay wt.-% from MultiMin, y-axis the number of points per bin (100 bins).

The bottom part of the Opalinus Clay (below 620 m), is more argillaceous: the mean and median dry clay content are close to 55.8 and 56.0 wt.-%.

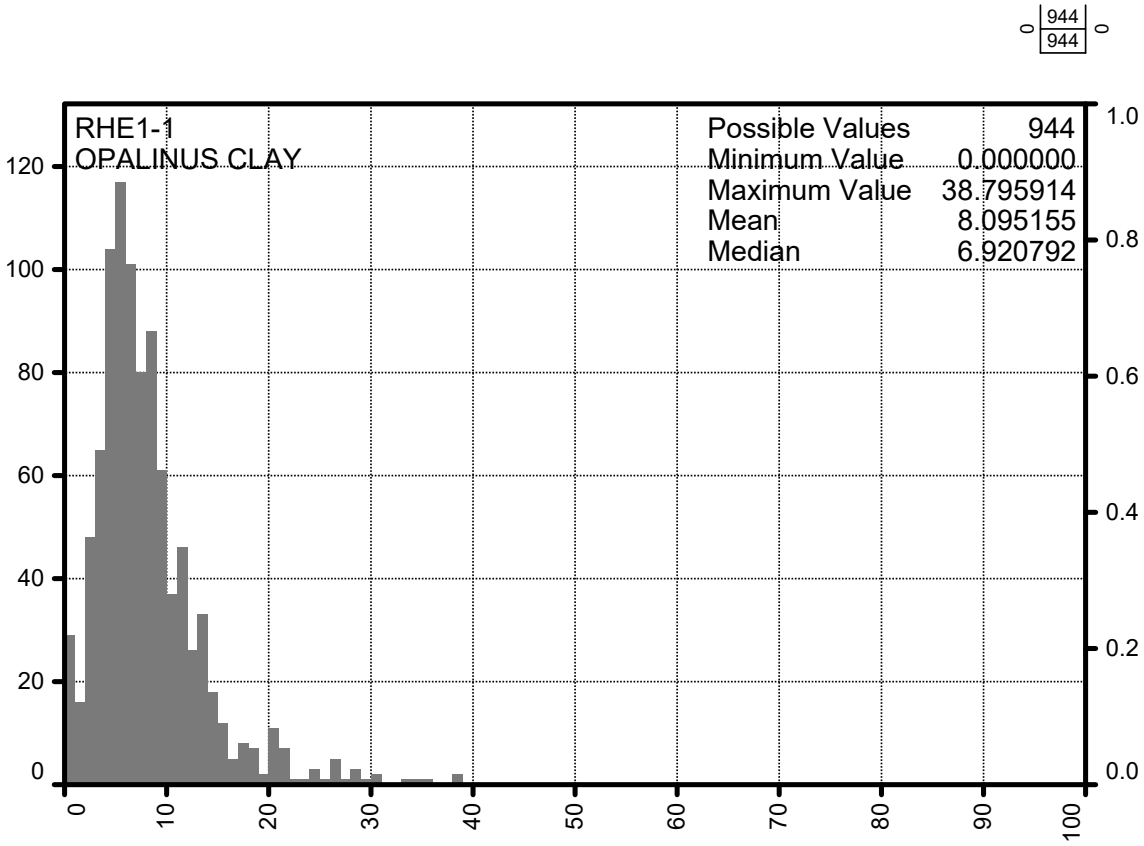

Fig. 4-4: Calcite weight-percentage frequency histogram in the Opalinus Clay

X-axis is the calcite wt.-% from MultiMin, y-axis the number of points per bin (100 bins).

The mean and median calcite content are close to 8.1 and 6.9 wt.-%. The maximum values are up to 38.8 wt.-%, i.e., corresponding to thin, calcite-rich layers. In case these layers are thinner than the log resolution, the maximum calcite content would be higher than computed by MultiMin.

The top part of the Opalinus Clay is slightly more calcitic than the bottom, see Plates 1 and 2.

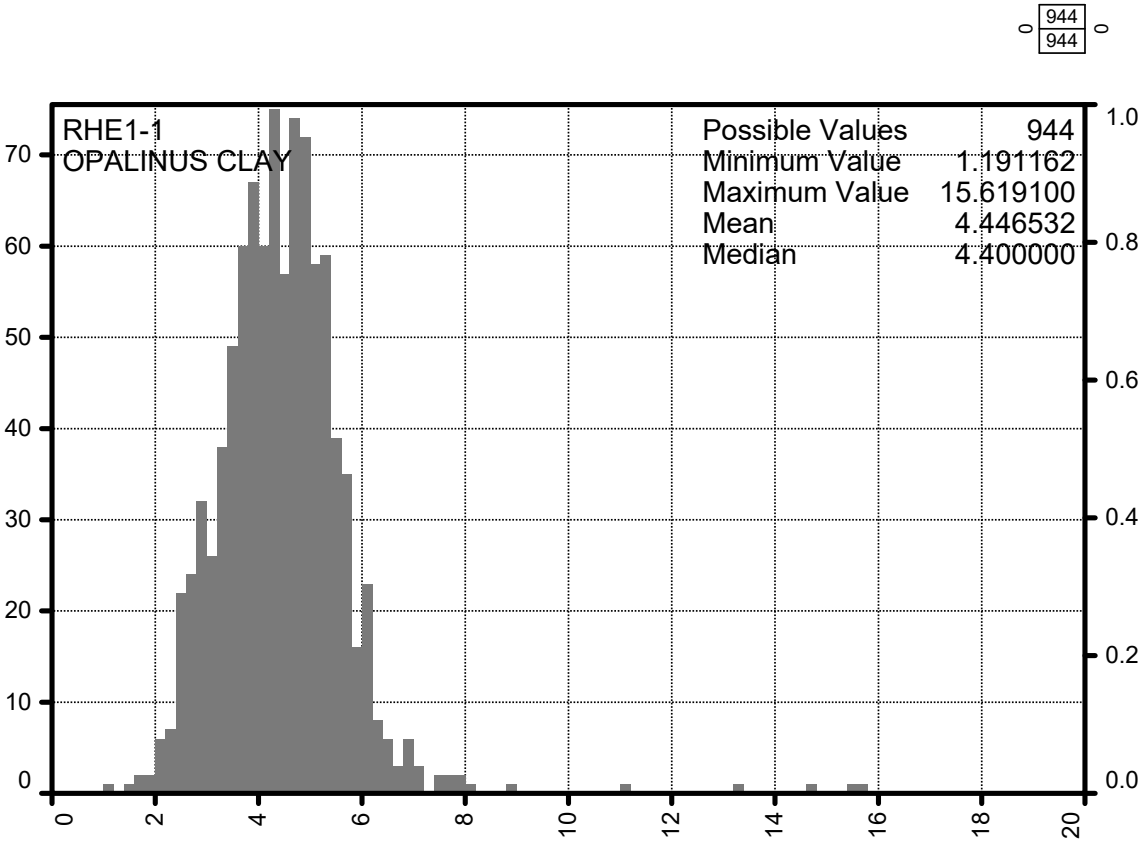

Fig. 4-5: Siderite weight-percentage frequency histogram in the Opalinus Clay

X-axis is the siderite wt.-% from MultiMin, y-axis the number of points per bin (100 bins).

The mean and median siderite content are close to 4.5 and 4.4 wt.-%, with a maximum value of 15.6 wt.-% and minimum values close to 1.2 wt.-%.

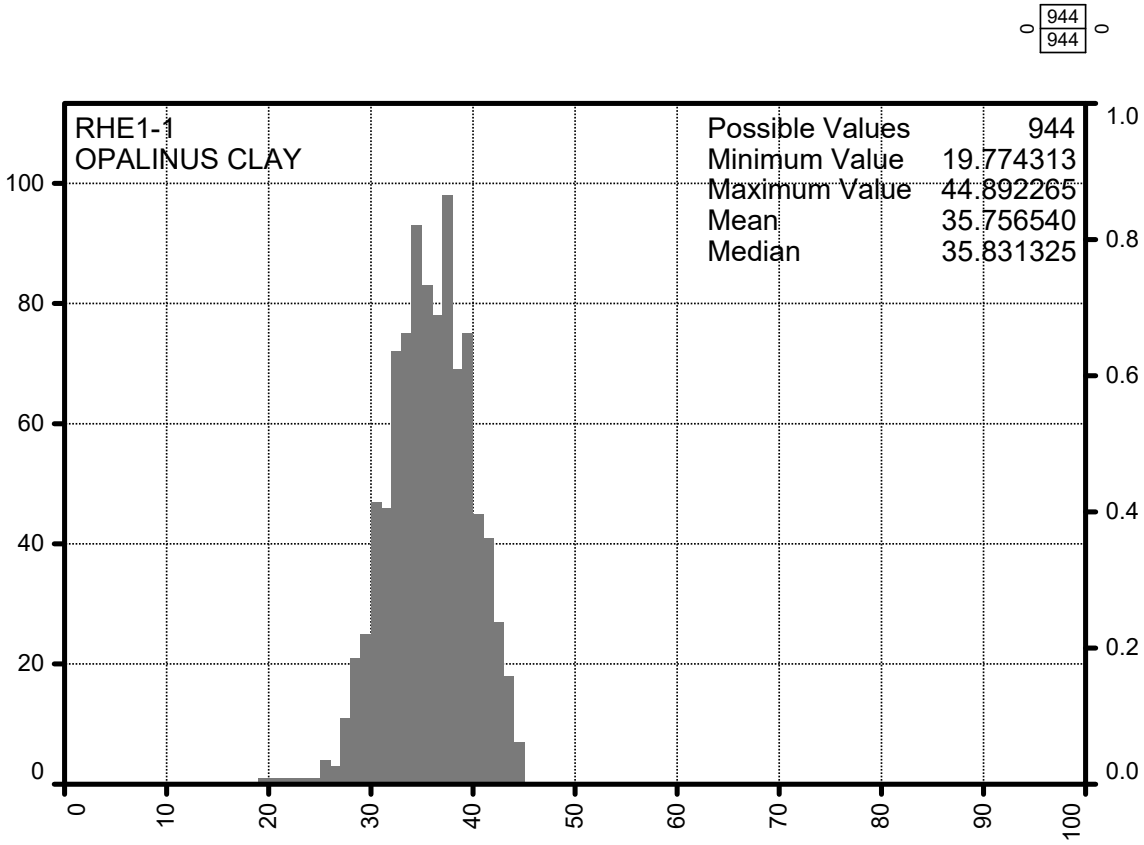

Fig. 4-6: QF-silicates (quartz and feldspars) weight percentage frequency histogram in the Opalinus Clay

X-axis is the QF-silicates wt.-% from MultiMin, y-axis the number of points per bin (100 bins).

The mean and median QF-silicates (quartz, plagioclases and potassic feldspars) contents are close to 35.8 wt.-%, much higher than for the carbonates (calcite close to 7 and 8 wt.-%).

The higher silicates content is located in the top part of the formation, see Plates 1 and 2.

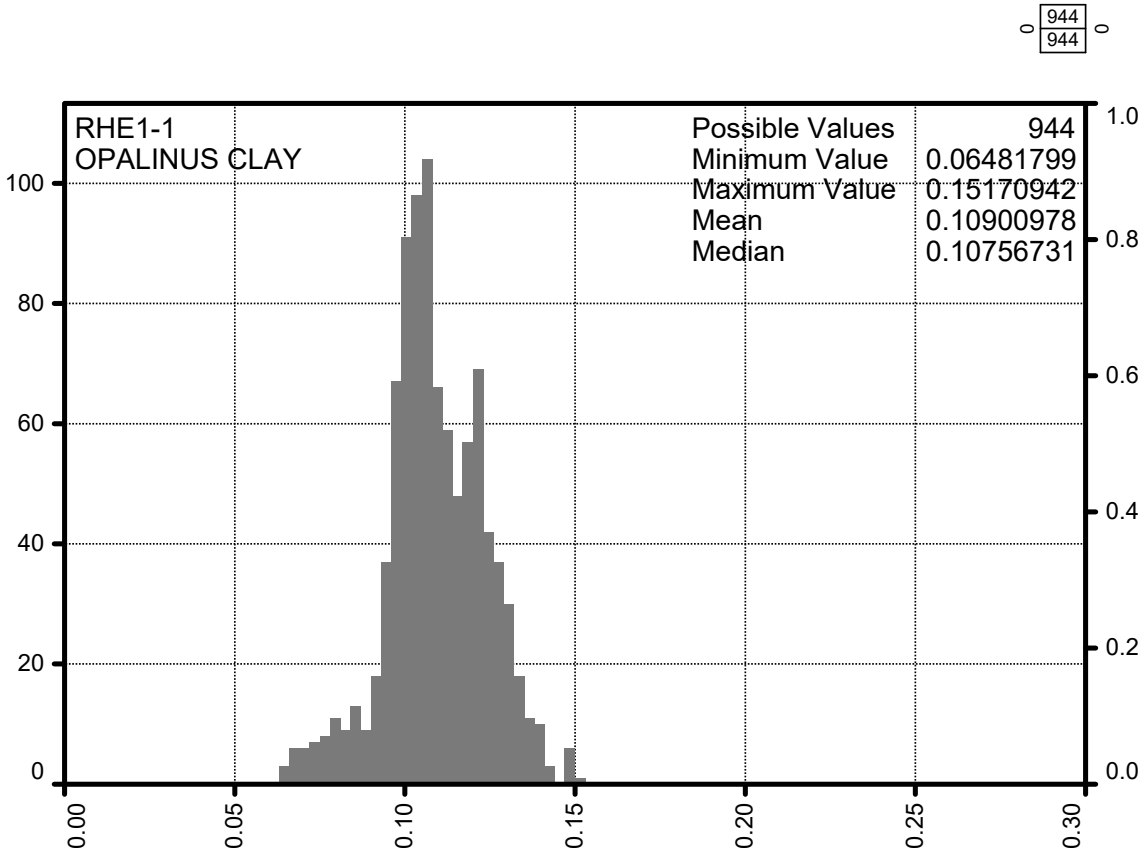

Fig. 4-7: Total porosity frequency histogram in the Opalinus Clay

X-axis is the total porosity v/v from MultiMin, y-axis the number of points per bin (100 bins).

The mean and median total porosities are close to 10.9 and 10.8%, with a range from 6.5 to 15.2%. The distribution is bimodal, reflecting the distribution of the clay content.

Fig. 4-8 below summarises the main results in the Opalinus Clay.

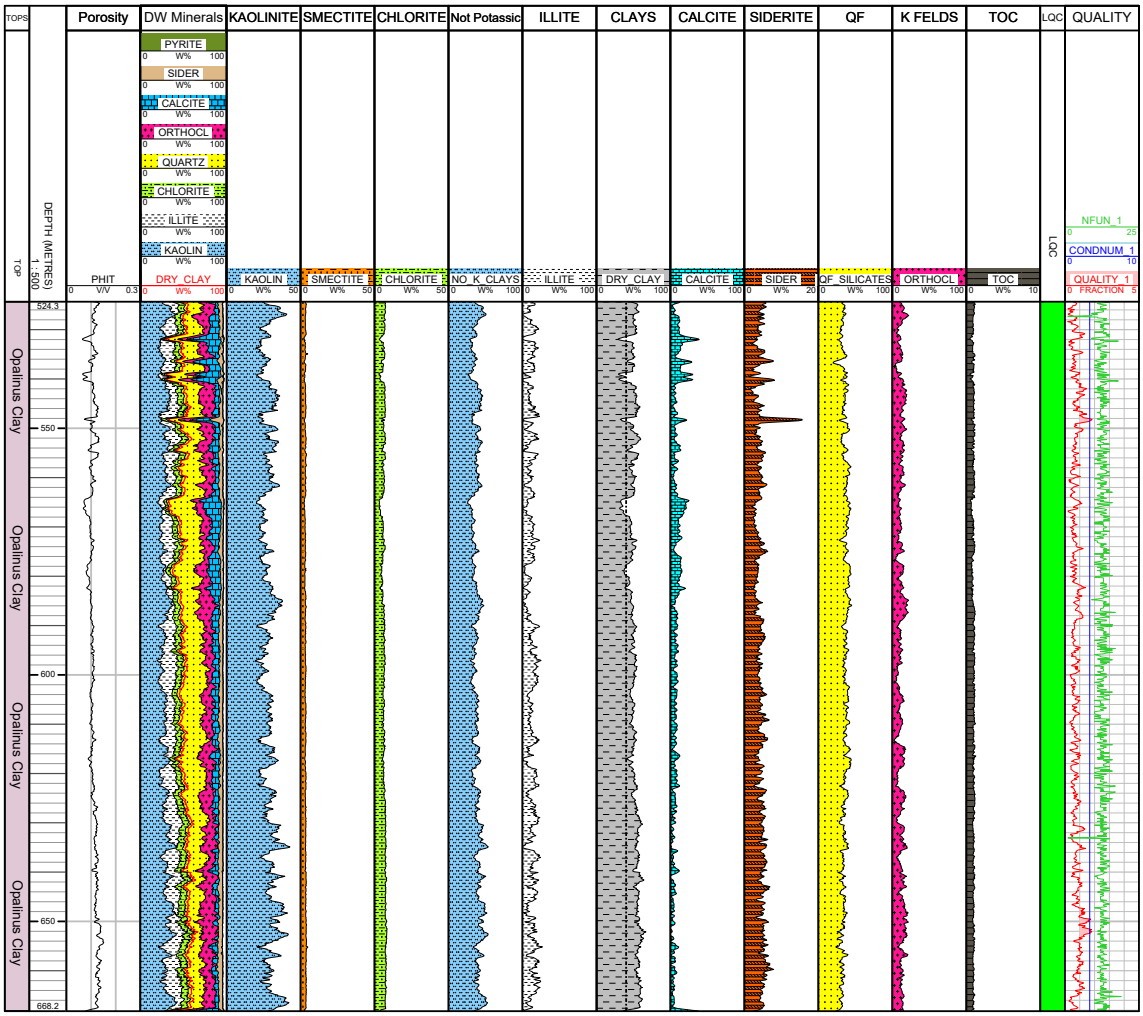

Fig. 4-8: Main log and core results in the Opalinus Clay

The dashed black line in the Clays track represents a 40 wt.-% baseline.

The wireline log quality was good in all the Opalinus Clay, as shown by the green LQC flag.

The MultiMin quality curve always remains low, generally below 1.00, indicating an overall good curve prediction.

The whole Opalinus Clay is very argillaceous, almost always above the 40 wt.-% (dashed black line in the "Clays" track in Fig. 4-8). A few carbonates streaks in the top third part have a lower clay content.

5 Summary

The MultiMin interpretation was successfully applied in the RHE1-1 borehole using the Paradigm Geolog MultiMin software (see Plates 1 and 2). Based on available petrophysical logs and formation mineralogical contents, several specific MultiMin interpretation intervals were identified. Some of these intervals needed to be further subdivided due to e.g. borehole conditions to ensure the best possible MultiMin interpretation result.

No core data from lab measurements were available, therefore the MultiMin results could not be checked against core data.

The mineralogical MultiMin interpretation results were converted to weight percentages, to be consistent with what was done in the other recent boreholes.

The clay typing was achieved using a clustering method (Facimage module of Geolog) for smectite and chlorites, and MultiMin for kaolinite and illite.

The continuous curves from the MultiMin interpretation can be used to characterise the different formations (and hence members) occurring in RHE1-1. The Opalinus Clay shows a variable total clay content though in most locations it is well above 40 wt.-%. The lower third of the formation is more argillaceous than the top, as already noticed in many regional locations.

In addition, boundaries between formations (and between members) are often clearly marked by a decrease or increase of clay-, QF-silicates and/or carbonate contents. The carbonate-rich formations can further be characterised according to the occurrence of dolomite (replacing calcite), especially in the lower part of the borehole (in the lithostratigraphic units of the Keuper). The measurement of the magnesium content with the ECS tool (MGWALK closure model) greatly supported the calcite – dolomite characterisation in these formations.

6 References

Birkhäuser, P., Roth, P., Meier, B. & Naef, H. (2001): 3D-Seismik: Räumliche Erkundung des mesozoischen Sedimentschichten im Zürcher Weinland. Nagra Technischer Bericht NTB 00-03.

Isler, A., Pasquier, F. & Huber, M. (1984): Geologische Karte der zentralen Nordschweiz 1:100'000. Herausgegeben von der Nagra und der Schweiz. Geol. Komm.

Jäggi, D., Laurich, B., Nussbaum, C., Schuster, K. & Connolly, P. (2017): Tectonic structure of the "Main Fault" in the Opalinus Clay, Mont Terri rock laboratory (Switzerland). Swiss Journal of Geosciences 110, 67-84.

Marnat, S. & Becker, J.K. (2021): Petrophysical log analyses of deep and shallow boreholes: methodology report. Nagra Arbeitsbericht NAB 20-30.

Mazurek, M. (2017): Gesteinsparameter-Datenbank Nordschweiz – Version 2. Nagra Arbeitsbericht NAB 17-56.

Nagra (2014): SGT Etappe 2: Vorschlag weiter zu untersuchender geologischer Standortgebiete mit zugehörigen Standortarealen für die Oberflächenanlage. Geologische Grundlagen. Dossier II: Sedimentologische und tektonische Verhältnisse. Nagra Technischer Bericht NTB 14-01.

Nagra (2019): Preliminary horizon and structure mapping of the Nagra 3D seismics ZNO-97/16 (Zürich Nordost) in time domain. Nagra Arbeitsbericht NAB 18-36.

Pietsch, J. & Jordan, P. (2014): Digitales Höhenmodell Basis Quartär der Nordschweiz – Version 2013 (SGT E2) und ausgewählte Auswertungen. Nagra Arbeitsbericht NAB 14-02.

Roche, V., Childs, C., Madritsch, H. & Camanni, G. (2020): Controls of sedimentary layering and structural inheritance on fault zone structure in three dimensions. A case study from the northern Molasse basin, Switzerland. Journal of the Geological Society 177/3, 493-508.

Waber, H.N. (ed.) (2020): SGT-E3 deep drilling campaign (TBO): Experiment procedures and analytical methods at RWI, University of Bern (Version 1.0, April 2020). Nagra Arbeitsbericht NAB 20-13.

Ye, S.J. & Rabiller, P. (2000): A new tool for electrofacies analysis: Multi-Resolution Graph-Based Clustering. SPWLA, 41st Annual Logging Symposium Transaction.